DISCRETE AND CONTINUOUS
DYNAMICAL SYSTEMS
Volume **13**, Number **4**, November **2005**

Website: http://aimSciences.org

pp. **843–876**

WAVE PROPAGATION AND BLOCKING IN INHOMOGENEOUS MEDIA

D.G. Aronson*, N.V. Mantzaris†, and H.G. Othmer‡

School of Mathematics
University of Minnesota
Minneapolis, MN 55455

Abstract. Wave propagation governed by reaction-diffusion equations in homogeneous media has been studied extensively, and initiation and propagation are well understood in scalar equations such as Fisher's equation and the bistable equation. However, in many biological applications the medium is inhomogeneous, and in one space dimension a typical model is a series of cells, within each of which the dynamics obey a reaction-diffusion equation, and which are coupled by reaction-free gap junctions. If the cell and gap sizes scale correctly such systems can be homogenized and the lowest order equation is the equation for a homogeneous medium [11]. However this usually cannot be done, as evidenced by the fact that such averaged equations cannot predict a finite range of propagation in an excitable system; once a wave is fully developed it propagates indefinitely. However, recent experimental results on calcium waves in numerous systems show that waves propagate though a fixed number of cells and then stop. In this paper we show how this can be understood within the framework of a very simple model for excitable systems.

1. **Introduction.** Until recently, astrocytes were considered passive bystanders in the brain, but it is now known that electrical, mechanical, and chemical stimuli can trigger complex intracellular calcium (Ca_i^{+2}) responses in these cells, both within a cell and on a scale of many cell lengths. Aggregates of cultured astrocytes can propagate waves that cross cell boundaries without decrement or delay, involve hundreds of cells, and last seconds to minutes [18]. Often waves originate at several points in a cell, each characterized by its own frequency and amplitude [19, 20], and often the waves from different loci interact and evolve into rotating spirals that involve many cells [4]. Ca_i^{+2} waves also arise in cardiac tissue, and it has been shown that spatial inhomogeneity in the release sites can block waves that would propagate in a spatially-uniform tissue [17].

Intercellular calcium waves require some form of cell-to-cell communication, and two major pathways have been identified: direct diffusion of inositol 1,4,5- trisphosphate (IP_3), and perhaps calcium, via gap junctions [3], and indirect communication via a secreted messenger released by stimulated cells [6]. Intercellular propagation involves gap junctions, because propagation is inhibited by gap junction blockers [5]. Communication is probably via diffusion of IP_3 through gap junctions, which generates Ca^{2+} release in one cell after another. It is not known whether these waves are regenerative, but it is often assumed that they are not because the waves

2000 *Mathematics Subject Classification.* 35Q80, 92B05.
Key words and phrases. wave block, inhomogeneous media, calcium waves, discrete systems.
*Also a member of the Institute for Mathematics and Its Applications, University of Minnesota
†Present address: Dept of Chemical and Biomolecular Engineering, Rice Univ, Houston, TX
‡Also a member of the Digital Technology Center, University of Minnesota

only propagate a short distance and stop [3]. Models based on passive diffusion of IP_3, IP_3-stimulated release of calcium, and communication via gap junctions have been developed [16], but the problem of predicting the extent of propagation remains unresolved. Our objective here is to analyze in detail a simplified model that can suggest an explanation for the finite range of propagation.

2. **Statement of the problem.** We consider the initial value problem for a bistable reaction-diffusion equation in a one-dimensional, non-homogeneous environment. Specifically, let $\mathfrak{P}$ denote the union of a finite number of disjoint finite open intervals on the real line, and let $\mathfrak{A}$ denote the interior of the complement of $\mathfrak{P}$. The differential equation is

$$v_t = D(x)v_{xx} + F(x,v),$$

where

$$D(x) = \begin{cases} D_a \text{ for } x \in \mathfrak{A} \\ D_p \text{ for } x \in \mathfrak{P} \end{cases},$$

and

$$F(x,v) = \begin{cases} f(v) & \text{for } x \in \mathfrak{A} \\ 0 & \text{for } x \in \mathfrak{P} \end{cases}.$$

For the initial value problem we impose the initial condition

$$v(\cdot,0) = v_0 \text{ in } \mathbf{R},$$

and the matching conditions

$$\begin{aligned} v(\cdot,t) &\in C(\mathbf{R}) \qquad \text{for all } t \geq 0 \\ D_p \lim_{\substack{x \to x_0 \\ x \in \mathfrak{P}}} v_x(x,t) &= D_a \lim_{\substack{x \to x_0 \\ x \in \mathfrak{A}}} v_x(x,t) \qquad \text{for all } t \geq 0 \text{ and } x_0 \in \overline{\mathfrak{A}} \cap \overline{\mathfrak{P}}. \end{aligned}$$

We will refer to $\mathfrak{A}$ as the *active region* and $\mathfrak{P}$ as the *passive region*. The individual intervals in $\mathfrak{P}$ will be called *gaps*.

This initial value problem has been studied for various choices of the reaction term $f(v)$. In the case $\mathfrak{P} = \emptyset$, Rinzel & Keller [13] deal with McKean's piecewise linear reaction term [8]

$$f(v) = \lambda \{H(v-a) - v\}, \tag{1}$$

where H is the Heaviside function, λ a positive parameter, and $a \in (0, 1/2)$ is the *threshold parameter*. They show that there is a traveling change-of state wave connecting the equilibria at $v \equiv 0$ and $v \equiv 1$. This solution is unique (up to translation) and (linearly) stable. When $\mathfrak{P}$ consists of a single interval, Snyed & Sherratt [15] show that if the gap is sufficiently large then there exist two monotone standing wave solutions, one stable and the other unstable. The stable solution can block transmission since for suitable initial data v_0 the solution to the initial value problem approaches the stable standing wave rather than either of the stable equilibria $v \equiv 0$ or $v \equiv 1$. Lewis & Keener [7] also find stable and unstable monotone standing wave solutions in the 1-gap problem for Nagumo's equation, i.e., with the smooth reaction term $f(v) = v(1-v)(v-a)$. In addition, they show that the standing waves emerge via a saddle-node bifurcation. Yang et al. [21] investigate Nagumo's equation numerically in the case in which $\mathfrak{P}$ contains more than one interval. In particular, they are interested in cases where the gaps are of different lengths and develop criteria for transmission and non-transmission when there are two or three gaps. In this paper we study the case of N gaps of equal length for the piecewise linear reaction term (1).

By a suitable rescaling of time and space we can eliminate all but two of the parameters and rewrite the initial value problem in the form

$$u_t = \begin{cases} u_{xx} + H(u-a) - u & \text{for } (x,t) \in \mathfrak{A} \times \mathbf{R}^+ \\ Du_{xx} & \text{for } (x,t) \in \mathfrak{P} \times \mathbf{R}^+ \end{cases}, \tag{2}$$

$$u(\cdot,0) = u_0 \text{ in } \mathbf{R},$$

$$u(\cdot,t), u_x(\cdot,t) \in C(\mathbf{R}) \text{ for all } t \geq 0,$$

where $D = D_a/D_p$.

Since the diffusivity and the reaction term in (2) are both discontinuous, the existence and uniqueness of solutions to the initial value problem is not obvious. However, by adapting the methods of Pauwelussen [12], who deals with discontinuous diffusivity, and of McKean [9], who deals with a non-smooth reaction term, one can prove the desired result. We omit the rather technical details and simply assume the result. Moreover, the discontinuity in the diffusivity does not play an essential role in our considerations, so to simplify the notation we will assume that $D = 1$ hereafter.

We consider the general case of N gaps of equal length γ separated by $N-1$ active intervals each of length β (Figure 1). We seek criteria for deciding when an initial datum u_0 for the initial value problem which is above threshold to the left of the first gap will generate a solution which ultimately fails to rise above threshold in one of the subsequent gaps or active regions. For this purpose we construct a sequence of monotone steady state (standing wave) solutions which cross threshold in one of the gaps or active regions. In particular, we construct standing waves which cross threshold in either the M^{th} gap or active interval for each $M = 1, ..., N$. In general, there do not exist standing wave solutions at all points in the (γ, β)-plane, so we will characterize the regions of existence for each choice of M and N. As we will see, these waves emerge in stable/unstable pairs. Waves which cross threshold in a gap are shown to be stable, while those which cross in an active region are unstable. These steady state solutions block transmission. For example, if the initial datum lies between two standing waves, one crossing threshold in the M^{th} active region and the other crossing in the $(M+1)^{st}$ with $M < N$ then the solution to the initial value problem will asymptotically approach a standing wave which crosses threshold in the $(M+1)^{st}$ gap. Roughly speaking, the space of initial functions is partitioned into three classes: one which generates solutions which ultimately die out, one which generates solutions which approach a traveling wave in the terminal active region, and one which generates solutions which approach non-trivial stationary patterns which are ultimately below threshold in the terminal active region.

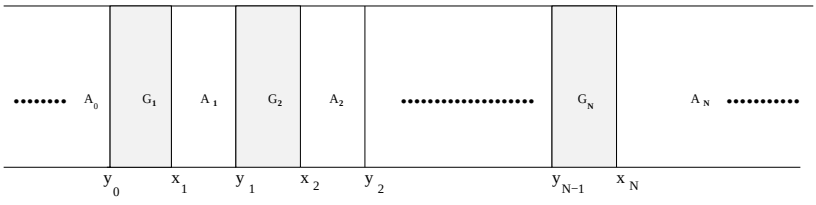

FIGURE 1. The geometry and labeling of the system.

Steady state solutions to (2) are solutions to the ordinary differential equation

$$u'' + I(x)\{H(u-a) - u\} = 0, \tag{3}$$

where

$$I(x) = \begin{cases} 0 \text{ if } x \in \mathfrak{P} \\ 1 \text{ if } x \in \mathfrak{A} \end{cases} .$$

In the phase plane, i.e., the (u, u')-plane, there are rest points at $\mathcal{O} = (0, 0)$ and $\mathcal{P} = (1, 0)$, both of which are saddles. We assume throughout that $a \in (0, 1/2)$. It is easy to show using first integrals that the stable and unstable manifolds of $\mathcal{O}$ coincide and form a homoclinic loop in the right half plane. The part of the loop in the fourth quadrant is given by

$$\begin{aligned} \Sigma_1 &: u' = -u \text{ for } 0 \le u \le a \\ \Sigma_2 &: u' = -\sqrt{u^2 - 2u + 2a} \text{ for } u > a. \end{aligned}$$

The branch in the fourth quadrant of the unstable manifold associated to $\mathcal{P}$ is given by

$$\Sigma_3 : u' = u - 1 \text{ for } 0 \le u \le 1.$$

These manifolds are shown in Figure 2. The steady state solutions we seek are monotone standing wave solutions which correspond in the phase plane to heteroclinic orbits from $\mathcal{P}$ to $\mathcal{O}$.

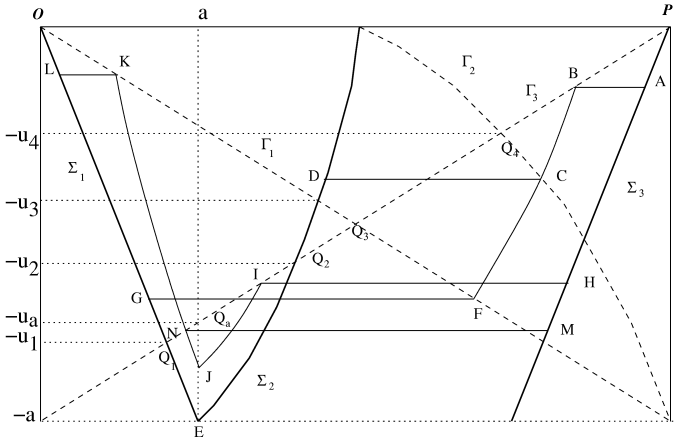

FIGURE 2. The phase plane for the two-gap problem with $\gamma > \gamma^* \equiv a^{-1} - 2$.

Although our construction of the standing wave solutions is analytic, in the case of two gaps it is possible to give a rather simple geometric construction which has the virtue of clearly displaying the admissible relationships between the lengths γ and β. We carry this out in Section 2. In Section 3 we turn to the general case $N \ge 1$ and carry out the formal construction of the standing wave solutions which cross the threshold value in the M^{th} gap for $M = 1, ..., N$. We make this construction rigorous in Section 4 by imposing the necessary constraints. We also explore the consequences of these constraints in determining the bifurcation curves and delineating the (γ, β) regions for the existence of standing waves. In Section 5 we investigate monotonicity properties with respect to M and N of the initial slope of a monotone standing wave solution which crosses threshold in the M^{th} gap of an N gap configuration. Standing waves which cross threshold in active regions are constructed in Section 6. The stability and instability of the various standing waves is studied in Section 7 using an extension of the comparison result of Pauwelussen

[12] and the convergence results of Aronson & Weinberger [1, 2]. In that Section we also discuss the pattern formation induced by the presence of gaps. Finally, in Section 8 we summarize our results and discuss various possible extensions.

3. **The geometric construction for the two-gap problem.** We consider the problem of constructing monotone standing waves in the presence of two gaps. We seek a C^1 solution to

$$u'' + H(u-a) - u = 0 \text{ for } x \in (-\infty, 0) \cup (\gamma, \gamma+\beta) \cup (2\gamma+\beta, \infty) \tag{4}$$

and

$$u'' = 0 \text{ on } (0,\gamma) \cup (\gamma+\beta, 2\gamma+\beta). \tag{5}$$

Since standing waves do not exist for all points in the (γ,β)-plane we proceed by fixing the gap length γ and determining the admissible values of the active region length β and the slope $-u^*$ at $x=0$.

To begin with we fix

$$\gamma > \gamma^* \equiv \frac{1}{a} - 2. \tag{6}$$

Integrating (4) with a given value of u' corresponds to traversing a horizontal segment of length $\gamma\,|u'|$ in the phase plane. The curves Γ_1, Γ_2 and Γ_3 in Figure 2 show the locus of phase points at a distance $\gamma\,|u'|$ from Σ_1, Σ_2, and Σ_3 respectively. Thus each point on Γ_j is the endpoint of a trajectory of (4) whose other endpoint lies on Σ_j for $j = 1, 2, 3$. The heteroclinic orbits we seek are constructed from segments of the manifolds Σ_1, Σ_2 and Σ_3, horizontal segments which are trajectories of (4), and curved segments which are trajectories of (4). These curved segments join Γ_3 to Γ_1 or to Γ_2, and determine the admissible values of β corresponding to the given value of γ.

The phase points

$$Q_j \equiv \begin{cases} \Gamma_3 \cap \Sigma_j \text{ for } j = 1,2 \\ \Gamma_3 \cap \Gamma_{j-2} \text{ for } j = 3,4 \end{cases}$$

and

$$Q_a \equiv \Gamma_3 \cap \{u = a\}$$

play a crucial role in determining the admissible values of β and u^*. Define the numbers u_j for $j = 1, .., 4$ by

$$Q_j \equiv (1 - (1+\gamma)u_j, -u_j)$$

and

$$u_a \equiv \frac{1-a}{1+\gamma}.$$

Then

$$a > u_1 > u_a > u_2 > u_3 > u_4 > 0.$$

For $0 < u^* < u_4$, where $(1-u^*, -u^*) \in \Sigma_3$, there are two families of heteroclinic orbits. One of these consists of orbits which cross threshold in the terminal active region, e.g., $\mathcal{P}\mathbf{ABCDE}\mathcal{O}$ in Figure 2. The curved segment $\widehat{\mathbf{BC}}$ represents a trajectory of (4) and determines an admissible active region length β. As $u^* \searrow 0$, $\widehat{\mathbf{BC}}$ approaches Σ_3 and $\beta \nearrow \infty$. As $u^* \nearrow u_4$, $\widehat{\mathbf{BC}}$ collapses to the point Q_4 and $\beta \searrow 0$. There are no heteroclinic orbits which cross threshold in the terminal active region for $u \geq u_4$.

Heteroclinic orbits in the other family cross threshold in the second gap. They exist for $0 < u^* < u_4$ and persist beyond $u^* = u_4$ for $u_4 \leq u^* < u_3$. An example is

$\mathcal{P}\mathbf{ABFG}\mathcal{O}$ in Figure 2. For these orbits the length β is determined by the curved segment $\widehat{\mathbf{BF}}$ with $\beta \searrow 0$ as $u^* \nearrow u_3$ and $\beta \nearrow \infty$ as $u^* \searrow 0$. The leftmost two curves in Figure 3 show β as a function of u^* for these two families of heteroclinic orbits.

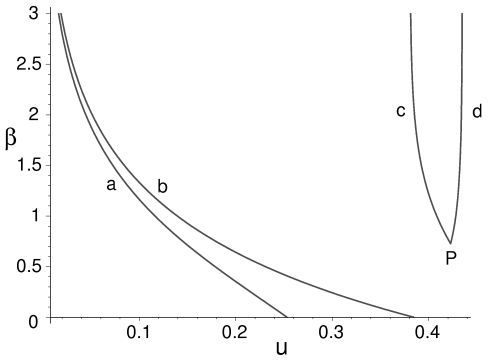

FIGURE 3. The (u, β)-plane for the two-gap problem with threshold $a = 0.45$ and gap length $\gamma = 0.3 > \gamma^* = 2/9$. Here $-u$ is the initial slope and β is the length of the intervals in the active region. For points (γ, β) on the curve labeled a (c) the corresponding standing wave solution crosses threshold in the active region A_2 (A_1). For points (γ, β) on the curve labeled b (d) the corresponding standing wave solution crosses threshold in the gap G_2 (G_1). The point labeled P is the minimum point (u_a, β_a).

For $u_2 < u^* < u_a$ there is a family of heteroclinic orbits which cross threshold in the active region A_1, e.g., $\mathcal{P}\mathbf{HIJKL}\mathcal{O}$ in Figure 2. The admissible values of β are determined by the trajectory $\widehat{IJK}$ of (4) with $\beta \nearrow \infty$ as $u^* \searrow u_2$. For $u_a < u^* < u_1$ there is a family of heteroclinic orbits which cross threshold in the first gap, e.g., $\mathcal{P}\mathbf{MNKL}\mathcal{O}$. Here the admissible values of β are determined by the trajectory $\widehat{\mathbf{NK}}$ of (4) with $\beta \nearrow \infty$ as $u^* \nearrow u_1$. When $u^* \to a$ the two families discussed here coalesce and there is a minimal value of β determined by the trajectory $\widehat{JK}$. The two rightmost curves in Figure 3 show β as a function of u^* for these two families. Note that the curves intersect at the point $(u^*, \beta) = (u_a, \beta_a)$, where β_a is the minimal allowable active region length for the given gap length γ. The point (u_a, β_a) is a bifurcation point in the sense that there are two distinct solution branches in its neighborhood.

When $\gamma = \gamma^*$ the intersection of Γ_3 and $\Sigma_1 \cup \Sigma_2$ is the single point $(a, -a)$, while for $\gamma < \gamma^*$ the intersection is empty. Thus there are no monotone standing waves which cross threshold in either the terminal active region or the second gap for $\gamma \leq \gamma^*$. However if

$$\frac{1}{2}\gamma^* < \gamma < \gamma^*$$

then Γ_1 and Γ_2 intersect the line $u' = -a$ in a point $\mathbf{C}$ (cf. Figure 4) whose u-coordinate lies in the interval $(a/2, 1-a)$. The trajectory of (4) which starts at $\mathbf{C}$ intersects Γ_3 in a point

$$\mathbf{B} \equiv (1 - (1+\gamma)u_b, -u_b)$$

where $u_b \in (0, a)$ with $u_b \searrow 0$ as $\gamma \to \gamma^*$ and $u_b \nearrow a$ as $\gamma \to \dfrac{1}{2}\gamma^*$.

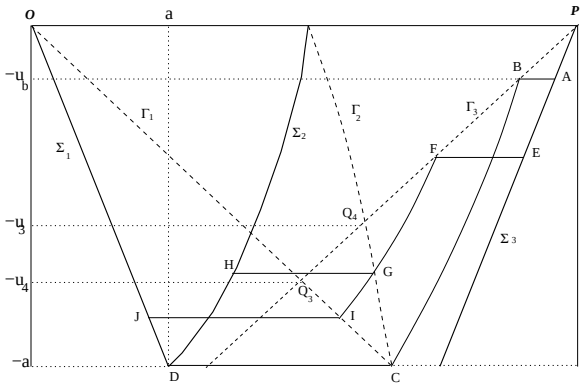

FIGURE 4. The phase plane for the two-gap problem with $\frac{\gamma^*}{2} < \gamma < \gamma^*$.

For $u_b < u^* < u_4$ there is a family of heteroclinic orbits which cross threshold in the terminal active region, e.g., $\mathcal{P}\mathbf{EFGHD}\mathcal{O}$ in Figure 4. For these orbits the length β of the active region is determined by the curve $\widehat{\mathbf{FG}}$ with $\beta \searrow 0$ as $u^* \nearrow u_4$. There are no heteroclinic orbits which cross threshold in the terminal active region for $u^* \geq u_4$.

For $u_3 < u^* < u_b$ there is a family of heteroclinic orbits which cross threshold in the second gap, e.g., $\mathcal{P}\mathbf{EFIJ}\mathcal{O}$ in Figure 4. For these trajectories the length β of the active region is determined by the curve $\widehat{\mathbf{FI}}$ with $\beta \searrow 0$ as $u^* \searrow u_3$. There are no heteroclinic orbits crossing threshold in the second gap for $u^* \leq u_3$.

The two families coincide at $u^* = u_b$ ($\mathcal{P}\mathbf{ABCD}\mathcal{O}$ in Figure 4) and there is a maximal value of $\beta = \beta_b$ (determined by the curve $\widehat{\mathbf{BC}}$) . Figure 5 shows β as a function of u^* for these two families. These curves intersect in a bifurcation point at $(u^*, \beta) = (u_b, \beta_b)$.

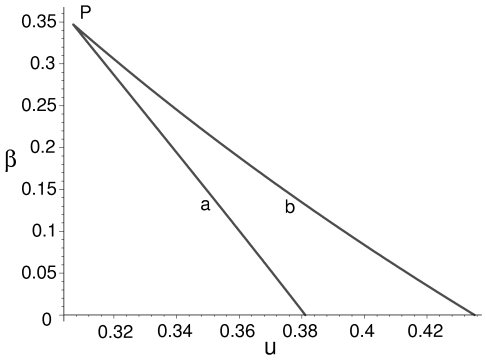

FIGURE 5. The (u, β)-plane for the two-gap problem with threshold $a = 0.45$ and gap length $\gamma = 0.15 \in (\frac{1}{2}\gamma^*, \gamma^*)$. Here $-u$ is the initial slope and β is the length of the intervals in the active region. For points (γ, β) on the curve labeled a (b) the corresponding standing wave solution crosses threshold in the active region A_2 (the gap G_2). The point labeled P is the maximum point (u_b, β_b).

The left-hand curve in Figure 6 shows the loci of the maxima $\beta = \beta_b(\gamma)$, and the right-hand curve shows the loci of the minima $\beta = \beta_a(\gamma)$ in the (γ, β)-plane. These curves are bifurcation curves in the sense that there exist two distinct solution branches for (γ, β)-values in the region to the right of them. The constructions described above establish the qualitative features of the graphs in Figures 3, 5, and 6. However, the figures actually show the results of computations which are described in Sections 4 and 6.

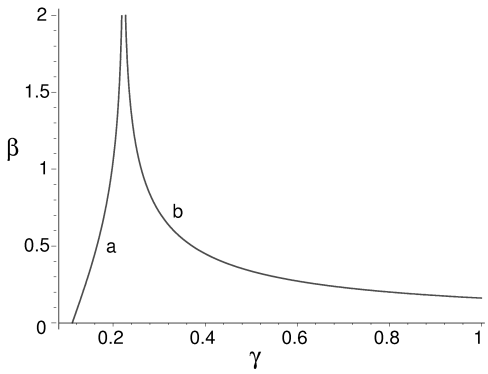

FIGURE 6. The (γ, β)-plane for the two-gap problem with threshold $a = 0.45$. The curve labeled a (b) is the locus of maximum (minimum) active region length $\beta = \beta_b(\gamma)$ ($\beta = \beta_a(\gamma)$).

4. **Solutions Which Cross Threshold in a Gap: Formal Construction.** We consider a configuration with N gaps each of length γ separated by $N-1$ active regions each of length β. The gaps are given by

$$G_j = (y_{j-1}, x_j) \text{ for } j = 1, ..., N$$

and the active regions are given by

$$A_0 = (-\infty, y_0), A_j = (x_j, y_j) \text{ for } j = 1, ..., N-1, \text{ and } A_N = (x_N, \infty),$$

where

$$x_j = j\gamma + (j-1)\beta \text{ and } y_j = j(\gamma + \beta)$$

(cf. Figure 1). We will give the formal construction of a monotone standing wave solution which crosses threshold in the gap G_M, where $1 \le M \le N$.

Let

$$U_j = \begin{pmatrix} u(x_j) \\ u'(x_j) \end{pmatrix} \text{ and } V_j = \begin{pmatrix} u(y_j) \\ u'(y_j) \end{pmatrix}.$$

In the gap G_j we integrate

$$u'' = 0$$

with initial value V_{j-1} to obtain

$$\begin{pmatrix} u(x) \\ u'(x) \end{pmatrix} = P(x - y_{j-1})V_{j-1},$$

where

$$P(z) = \begin{pmatrix} 1 & z \\ 0 & 1 \end{pmatrix}.$$

In particular, at the end of G_j we have

$$U_j = PV_{j-1},$$

where

$$P = P(\gamma) = \begin{pmatrix} 1 & \gamma \\ 0 & 1 \end{pmatrix}.$$

If $j < M$ we are above threshold so that in A_j we integrate

$$u'' - u + 1 = 0$$

with initial value U_j to obtain

$$\begin{pmatrix} u(x) \\ u'(x) \end{pmatrix} - \epsilon_1 = A(x - x_j)(U_j - \epsilon_1),$$

where

$$A(z) = \begin{pmatrix} \cosh z & \sinh z \\ \sinh z & \cosh z \end{pmatrix} \text{ and } \epsilon_1 = \begin{pmatrix} 1 \\ 0 \end{pmatrix}.$$

Thus at the end of A_j we have

$$V_j - \epsilon_1 = A(PV_{j-1} - \epsilon_1), \tag{7}$$

where

$$A = A(\beta) = \begin{pmatrix} \cosh \beta & \sinh \beta \\ \sinh \beta & \cosh \beta \end{pmatrix}.$$

For the first gap the left-hand endpoint must lie on the unstable manifold of the rest point $\mathcal{P} = (1, 0)$ in A_0. Write

$$V_0 = \begin{pmatrix} 1 - u^* \\ -u^* \end{pmatrix}.$$

Then

$$U_1 = PV_0 = \epsilon_1 - u^* P\epsilon,$$

where

$$\epsilon = \begin{pmatrix} 1 \\ 1 \end{pmatrix},$$

and

$$V_1 - \epsilon_1 = -u^* AP\epsilon. \tag{8}$$

In view of (8), iteration of (7) yields

$$V_{M-1} - \epsilon_1 = -u^*(AP)^{M-1}\epsilon,$$

and crossing G_M we find

$$U_{M-1} = \epsilon_1 - u^* P(AP)^{M-1}\epsilon$$

since $P\epsilon_1 = \epsilon_1$.

Since we assume that the threshold $u = a$ is crossed in G_M the Heaviside function in (3) is zero, we proceed by integrating

$$u'' - u = 0$$

across A_M to obtain

$$V_M = A\epsilon_1 - u^*(AP)^M\epsilon$$

and

$$U_{M+1} = PA\epsilon_1 - u^* P(AP)^M\epsilon.$$

Continuing in this manner successively applying A and P yields

$$U_N = (PA)^{N-M}\epsilon_1 - u^* P(AP)^{N-1}\epsilon$$

at the end of the final gap G_N. The stable manifold of $\mathcal{O}$ is given by $u + u' = 0$. Since U_N must lie on this manifold we have

$$0 = \epsilon^T U_N = \epsilon^T (PA)^{N-M} \epsilon_1 - u^* \epsilon^T P (AP)^{N-1} \epsilon$$

so that

$$u^* = u^*_{MN} = \frac{\epsilon^T (PA)^{N-M} \epsilon_1}{\epsilon^T P (AP)^{N-1} \epsilon}. \tag{9}$$

Note that (9) can also be written in the form

$$u^*_{MN} = \frac{\epsilon^T (PA)^{N-M} \epsilon_1}{\epsilon^T (PA)^{k-1} P (AP)^{N-k} \epsilon} \text{ for } k = 1, ..., N. \tag{10}$$

To simplify (10), we write

$$(AP)^k \epsilon = \begin{pmatrix} f_k \\ g_k \end{pmatrix}, \tag{11}$$

where

$$AP = \begin{pmatrix} \cosh(\beta) & \sinh(\beta) + \gamma \cosh(\beta) \\ \sinh(\beta) & \cosh(\beta) + \gamma \sinh(\beta) \end{pmatrix}.$$

Note that $f_0 = g_0 = 1$, and that f_k and g_k are positive for all integers k. Moreover,

$$f_{k+1} > f_k \text{ and } g_{k+1} > g_k. \tag{12}$$

Since

$$(PA)^k = \begin{pmatrix} 0 & 1 \\ 1 & 0 \end{pmatrix} \left((AP)^k\right)^T \begin{pmatrix} 0 & 1 \\ 1 & 0 \end{pmatrix}$$

it follows that

$$\epsilon^T (PA)^k = \begin{pmatrix} g_k & f_k \end{pmatrix}. \tag{13}$$

Thus we can rewrite (10) as

$$u^*_{MN} = \frac{g_{N-M}}{g_{k-1}(f_{N-k} + \gamma g_{N-k}) + f_{k-1} g_{N-k}} \text{ for } k = 1, ..., N. \tag{14}$$

Note that (14) implies that

$$g_{k-1}(f_{N-k} + \gamma g_{N-k}) + f_{k-1} g_{N-k} = g_{j-1}(f_{N-j} + \gamma g_{N-j}) + f_{j-1} g_{N-j} \text{ for all } k, j. \tag{15}$$

Once u^* is known, the monotone standing wave is uniquely determined, at least formally. In particular

$$\begin{pmatrix} u \\ u' \end{pmatrix} = \begin{cases} \epsilon_1 - u^* P (x - y_{k-1}) (AP)^{k-1} \epsilon \text{ for } x \in G_k,\ k \le M \\ \epsilon_1 - u^* A (x - x_k) P (AP)^{k-1} \epsilon \text{ for } x \in A_k,\ k \le M - 1 \\ A(x - x_k)\{(PA)^{k-M} \epsilon - u^* P (AP)^{k-1} \epsilon\} \text{ for } x \in A_k,\ M \le k \le N - 1 \\ P(x - x_k)\{A(PA)^{k-M} \epsilon - u^* (AP)^k \epsilon\} \text{ for } x \in G_k, M \le k \le N \end{cases}. \tag{16}$$

Note that formally the function defined by (16) is a steady state solution on $[0, x_N]$ which crosses threshold in the Mth gap. However, it is not a standing wave unless $u^* = u^*_{MN}$.

5. **Constraints.** The derivation of the formulae (14) for u^*_{MN} given in the previous section is purely formal. Although it is assumed that the threshold is crossed in the M^{th} gap, u^*_{MN} as given by (14) is in fact independent of the value of the threshold parameter a. Hence there is no guarantee that this crossing actually occurs for any *preassigned* value of a. To ensure a crossing we must apply various constrains which depend on the actual value of a.

In the gap G_M the solution starts at the phase point $(1-u^*_{MN}f_{M-1}, -u^*_{MN}g_{M-1})$. Since this point must not lie below threshold we must require that $1-u^*_{MN}f_{M-1} \geq a$, i.e.,

$$u^*_{MN} \leq \frac{1-a}{f_{M-1}}.$$

Using (13) with $L = N - M + 1$ this is equivalent to

$$X_{MN}(\gamma,\beta) \equiv (\frac{1}{a} - 1)g_{M-1}(f_{N-M} + \gamma g_{N-M}) - f_{M-1}g_{N-M} \geq 0. \tag{17}$$

Equality in (17) occurs exactly when the solution crosses threshold at the beginning of the G_M or, equivalently, at the end of the A_{M-1}. Moreover, the phase point $(1-u^*_{MN}f_{M-1}, -u^*_{MN}g_{M-1})$ must lie above the line $u' = -a$. Hence we must have $-u^*_{MN}g_M > -a$ or

$$u^*_{MN} < \frac{a}{g_{M-1}}.$$

An equivalent form of this condition is

$$Y_{MN}(\gamma,\beta) \equiv g_{N-M}(f_{M-1} + \gamma g_{M-1}) + g_{M-1}(f_{N-M} - \frac{1}{a}g_{N-M}) \geq 0. \tag{18}$$

In the gap G_M the solution ends at the phase point

$$(1 - u^*_{MN}(f_{M-1} + \gamma g_{M-1}), -u^*_{MN}g_{M-1}).$$

This point must lie on or to the left of $u = a$ and either on the stable manifold of $\mathbf{0}$ if $M = N$ or to the right of it if $M < N$. Thus

$$u^*_{MN}g_{M-1} \leq 1 - u^*_{MN}(f_{M-1} + \gamma g_{M-1}) \leq a \tag{19}$$

with equality on the left if and only if $M = N$.

The left hand inequality in (19) is always satisfied. To see this observe that, in view of (14) with $k = N - M + 1$, this inequality is equivalent to

$$g_{M-1}(f_{N-M+1} - g_{N-M+1}) \geq 0.$$

Since $g_k > 0$ it suffices to prove that

$$f_k - g_k > 0 \text{ for all integers } k \geq 1. \tag{20}$$

We do this by induction. For $k = 1$

$$f_1 - g_1 = \gamma(\cosh\beta - \sinh\beta) > 0.$$

Write

$$(AP)^k = \begin{pmatrix} m_{11} & m_{12} \\ m_{21} & m_{22} \end{pmatrix},$$

where the $m_{ij} > 0$. Then $f_k = m_{11} + m_{12}$, $g_k = m_{21} + m_{22}$, and we assume that $f_k - g_k > 0$. Now

$$(AP)^{k+1} =$$

$$\begin{pmatrix} m_{11}\cosh\beta + m_{21}(\sinh\beta + \gamma\cosh\beta) & m_{12}\cosh\beta + m_{22}(\sinh\beta + \gamma\cosh\beta) \\ m_{11}\sinh\beta + m_{22}(\cosh\beta + \gamma\sinh\beta) & m_{12}\sinh\beta + m_{22}(\cosh\beta + \gamma\sinh\beta) \end{pmatrix}$$

so that

$$f_{k+1} - g_{k+1} = (f_k - g_k + \gamma g_k)\,(\cosh\beta - \sinh\beta) > 0,$$

which proves the assertion.

The right hand inequality in (19) is equivalent to

$$u^*_{MN} > \frac{1-a}{f_{M-1} + \gamma g_{M-1}}$$

or

$$Z_{MN}(\gamma,\beta) \equiv g_{N-M}(f_{M-1} + \gamma g_{M-1}) + (1 - \frac{1}{a}) f_{N-M} g_{M-1} \geq 0. \tag{21}$$

Note that equality in (21) occurs exactly when the solution crosses threshold at the end of G_M or equivalently at the beginning of A_M.

For the existence of a monotone standing wave solution which crosses threshold in the M^{th} gap it is necessary and sufficient that (γ,β) be such that (17), (18), and (21) are simultaneously satisfied. In view of (18) and (21) we have

$$Y_{MN} = Z_{MN} + \frac{1}{a} g_{M-1}(f_{N-M} - g_{N-M}).$$

Since $Y_{NN} = 0$ and $Z_{MN} = 0$ coincide, it follows from (20) that

$$Y_{MN} \geq \ Z_{MN} \text{ with equality only for } M = N.$$

Therefore $Y_{MN} \geq 0$ whenever $Z_{MN} \geq 0$, and in particular, (18) is automatically satisfied whenever (21) holds. Thus the condition (18) is redundant. The region in the $(\gamma,\beta)-$plane where (17) and (21) both hold is delineated by the sets where $X_{MN}(\gamma,\beta)$ and $Z_{NM}(\gamma,\beta)$ vanish. The coincidence of $Y_{NN} = 0$ and $Z_{NN} = 0$ means that the phase point at the end of the N^{th} gap has coordinates $(a,-a)$.

In the two-gap case discussed in Section 2, the curves $\beta = \beta_a(\gamma)$ and $\beta = \beta_b(\gamma)$ in Figure 6 are, respectively, the curves $Z_{12} = 0$ and $Z_{22} = 0$. Figure 7 shows the curves $X_{M5} = 0$ and $Z_{M5} = 0$ for two different values of the threshold parameter a and for various values of $M \in \{1,...,5\}$. As we noted above, the curves $X_{MN} = 0$ and $Z_{MN} = 0$ describe the loci of points in the (γ,β)-plane where the crossing of the threshold occurs at the intersection of an active and a passive region. As in the two-gap case, we expect these points to be bifurcation points where branches of solutions crossing in an active and in a passive region meet. This will be discussed in Section 6.

We investigate the sets where $X_{MN}(\gamma,\beta) = 0$ and $Z_{NM}(\gamma,\beta) = 0$. Since

$$A(\beta)P(0) = \begin{pmatrix} \cosh\beta & \sinh\beta \\ \sinh\beta & \cosh\beta \end{pmatrix}$$

we have

$$\begin{pmatrix} f_k(0,\beta) \\ g_k(0,\beta) \end{pmatrix} = (\cosh\beta + \sinh\beta)^k \mathbf{e}.$$

Therefore

$$X_{MN}(0,\beta) = \gamma^*(\cosh\beta + \sinh\beta)^{N-1} > 0 \tag{22}$$

and

$$Z_{NM}(0,\beta) = -\gamma^*(\cosh\beta + \sinh\beta)^{N-1} < 0, \tag{23}$$

where

$$\gamma^* = \frac{1}{a} - 2.$$

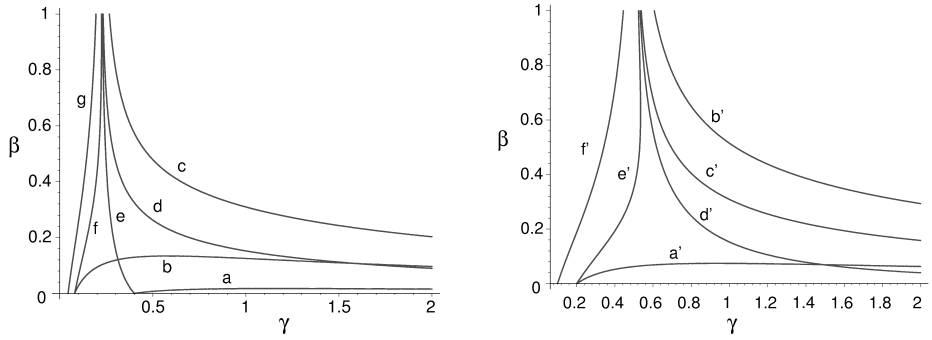

FIGURE 7. (a) The (γ, β)-plane for the five-gap problem with threshold $a = 0.45$. The curve labeled a is $X_{45} = 0$, b is $X_{55} = 0$, c is $Z_{15} = 0$, d is $Z_{25} = 0$, e is $Z_{35} = 0$, f is $Z_{45} = 0$, and g is $Z_{55} = 0$. For $a = 0.45$, $X_{M5} \neq 0$ in the first quadrant for $M = 1, 2$,or 3. (b) The (γ, β)-plane for the five-gap problem with threshold $a = 0.4$. The curve labeled a is $X_{55} = 0$, b is $Z_{15} = 0$, c is $Z_{25} = 0$, d is $Z_{35} = 0$, e is $Z_{45} = 0$, and f is $Z_{45} = 0$. For $a = 0.4$, $X_{M5} \neq 0$ in the first quadrant for $M = 1, 2, 3$ or 4.

For fixed β and $\gamma \gg 1$

$$A(\beta)P(\gamma) \sim \gamma \begin{pmatrix} 0 & \cosh\beta \\ 0 & \sinh\beta \end{pmatrix}$$

so that

$$\begin{pmatrix} f_k(\gamma,\beta) \\ g_k(\gamma,\beta) \end{pmatrix} \sim \gamma^k (\sinh\beta)^{k-1} \begin{pmatrix} \cosh\beta \\ \sinh\beta \end{pmatrix} \text{ as } \gamma \to \infty.$$

It follows that

$$X_{MN}(\gamma,\beta) \sim (\frac{1}{a} - 1)\gamma^N (\sinh\beta)^{N-1} > 0 \text{ as } \gamma \to \infty \tag{24}$$

and

$$Z_{NM}(\gamma,\beta) \sim \gamma^N (\sinh\beta)^{N-1} > 0 \text{ as } \gamma \to \infty. \tag{25}$$

Since

$$(A(0)P(\gamma))^k = \begin{pmatrix} 1 & \gamma \\ 0 & 1 \end{pmatrix}^k = \begin{pmatrix} 1 & k\gamma \\ 0 & 1 \end{pmatrix}$$

we have

$$\begin{pmatrix} f_k(\gamma,0) \\ g_k(\gamma,0) \end{pmatrix} = \begin{pmatrix} 1+k\gamma \\ 1 \end{pmatrix}.$$

Hence

$$X_{MN}(\gamma,0) = \gamma^* + \frac{\gamma}{a}(N_a - M + 1)$$

and

$$Z_{MN}(\gamma,0) = -\gamma^* - \frac{\gamma}{a}(N_a - M),$$

where

$$N_a \equiv (1-a)N.$$

We conclude that

$$X_{MN}(\gamma,0) \begin{cases} > 0 \text{ if } 0 \le \gamma < \gamma_{M-1,N} \\ < 0 \text{ if } \gamma > \gamma_{M-1,N} \end{cases} \tag{26}$$

and

$$Z_{MN}(\gamma,0)\begin{cases} <0 \text{ if } 0\le\gamma<\gamma_{MN} \\ >0 \text{ if } \gamma>\gamma_{MN}\end{cases}, \tag{27}$$

where

$$\gamma_{MN}=\begin{cases} +\infty \text{ if } M\le N_a \\ \dfrac{1-2a}{M-N_a} \text{ if } M>N_a\end{cases}.$$

In Appendix A we show that

$$X_{MN}(\gamma,\beta)\sim(\gamma^*+(\frac{1}{a}-1)\gamma)(2+\gamma)^{N-1}\left(\frac{e^\beta}{2}\right)^{N-1}>0 \text{ as } \beta\to\infty, \tag{28}$$

$$Z_{MN}(\gamma,\beta)\sim(2+\gamma)^{N-1}(\gamma-\gamma^*)\left(\frac{e^\beta}{2}\right)^{N-1} \text{ as } \beta\to\infty, \tag{29}$$

and

$$Z_{MN}(\gamma^*,\beta)\sim\gamma^*(2+\gamma^*)^{N-2}\frac{e^{(N-3)\beta}}{2^{N-2}}\times\begin{cases} 1 & \text{if } M=N \\ \left(2-\dfrac{1}{a}\right)<0 & \text{if } 2\le M\le N-1 \\ \left(1-\dfrac{1}{a}\right)<0 & \text{if } M=1\end{cases} \tag{30}$$

as $\beta\to\infty$.

¿From (23) and (25) we see that for each $\beta>0$ there is at least one root of $Z_{MN}(\gamma,\beta)=0$ in $\mathbf{R}^+$. Let $\gamma=\zeta_{MN}(\beta)$ denote the smallest such root. Generically we would expect the graph of $\gamma=\zeta_{MN}(\beta)$ to consist of a number of disjoint arcs. However, all of our numerical studies (cf. Figure 7) indicate that it is a smooth curve and that there are no additional roots in the first quadrant. To simplify the discussion we will assume that this is indeed the case.

We can say more about the set $Z_{NN}=0$ for large N. At the end of G_N we have

$$\begin{pmatrix} a \\ -a\end{pmatrix}=\epsilon_1-u^*_{NN}(PA)^{N-1}P\epsilon,$$

where $u^*_{NN}(\gamma,\beta)$ is defined by

$$u^*_{NN}=\frac{1-a}{\epsilon_1^T(PA)^{N-1}P\epsilon}.$$

Let

$$\epsilon_2=\begin{pmatrix} 0 \\ 1\end{pmatrix}.$$

The equation

$$a=u^*_{NN}\epsilon_2^T(PA)^{N-1}P\epsilon$$

establishes a relationship between γ and β. In particular

$$\frac{1}{a}-1=\frac{\epsilon_1^T(PA)^{N-1}P\epsilon}{\epsilon_2^T(PA)^{N-1}P\epsilon}.$$

The eigenvalues of PA are

$$\lambda_j=\frac{1}{2}\left(2\cosh\beta+\gamma\sinh\beta+(-1)^j\sqrt{(2\cosh\beta+\gamma\sinh\beta)^2-4}\right) \text{ for } j=1,2$$

and the corresponding eigenvalues are

$$v_j = \begin{pmatrix} \dfrac{\lambda_2 - \cosh\beta}{\sinh\beta} \\ 1 \end{pmatrix}.$$

Note that $\lambda_1\lambda_2 = 1$ and $0 < \lambda_1 < 1 < \lambda_2$. Write

$$P\epsilon = c_1 v_1 + c_2 v_2,$$

where the c_j depend on γ, β, and N. Then

$$(PA)^{N-1} P\epsilon = c_1\lambda_1^{N-1} v_1 + c_2\lambda_2^{N-1} v_2$$

and

$$\frac{1}{a} - 1 = \frac{c_1\lambda_1^{N-1}\epsilon_1^T v_1 + c_2\lambda_2^{N-1}\epsilon_1^T v_2}{c_1\lambda_1^{N-1}\epsilon_2^T v_1 + c_2\lambda_2^{N-1}\epsilon_2^T v_2}.$$

Therefore

$$\frac{1}{a} - 1 = \frac{\lambda_2 - \cosh\beta}{\sinh\beta} + \mathcal{O}(\rho^{N-1}),$$

where $\rho = \lambda_1/\lambda_2 < 1$. It follows that

$$\gamma_{NN}(\beta) = \frac{\alpha^2 - 1}{\alpha + \coth\beta} + \mathcal{O}(\rho^{N-1}),$$

where $\alpha = \dfrac{1}{a} - 1$. In particular, the limiting position of $\gamma = \gamma_{NN}(\beta)$ is given by

$$\gamma_\infty(\beta) = \lim_{N\to\infty} \gamma_{NN}(\beta) = \frac{\alpha^2 - 1}{\alpha + \coth\beta}$$

and for each fixed β the convergence is exponential. Moreover,

$$\lim_{\beta\to\infty} \gamma_\infty(\beta) = \gamma^*.$$

Figure 8 is a schematic representation of the first quadrant of the $(\gamma, \beta)-$plane as a finite rectangle. In this representation the upper and right hand sides of the rectangle represent $\beta = \infty$ and $\gamma = \infty$ respectively. According to (23) and (27), if $M \le N_a$ then $Z_{MN} < 0$ on the left hand and lower boundaries of the rectangle, and this is indicated by the dashed lines. From (25) we see that $Z_{MN} > 0$ on the right hand boundary and this is indicated with a heavy solid line. On the top of the rectangle, in view of (27), $Z_{MN} < 0$ for $\gamma < \gamma^*$ and > 0 for $\gamma > \gamma^*$. Finally, from (28) we see that $Z_{MN}(\gamma^*, \beta) < 0$ for $\beta \to \infty$. The curve $\gamma = \zeta_{MN}(\beta)$ must contain the points $\alpha = (\gamma^*, \infty)$ and $\omega = (\infty, 0)$ where Z_{MN} changes sign and must approach α from the right, as indicated in the figure. The part of the curve between these points is drawn to agree with our numerical observations (cf. Figure 7).

Figures 9(a) and 9(b) are schematic representations of $\gamma = \zeta_{MN}(\beta)$ for $N_a < M < N$ with the same conventions we have used in Figure 8. Here $\omega = (\gamma_{MN}, 0)$. Since $\gamma = \zeta_{MN}(\beta)$ must still approach α from the right as $\beta \to \infty$, it must cross the line $\gamma = \gamma^*$ in case $\zeta_{MN}(0) = \gamma_{MN} < \gamma^*$ as shown in Figure 9(a). When this occurs, corresponding to gap lengths $\gamma > \gamma^*$ which are sufficiently close to γ^*, there are at least two values of β for which $Z_{MN}(\gamma, \beta) = 0$. For $M = N$, we have $\gamma_{NN} = \gamma^*/N$. Moreover, it follows from (28) that $\gamma = \zeta_{MN}(\beta)$ must approach α from the left. This is shown in Figure 10.

If $M \le N_a + 1$ then according to (22), (23), (24) and (26) $X_{MN} > 0$ everywhere on the boundary of the rectangle representing the first quadrant of the $(\gamma, \beta)-$plane. Thus for any fixed $\gamma > 0$ we expect that $X_{MN}(\gamma, \beta) = 0$ has an even number of

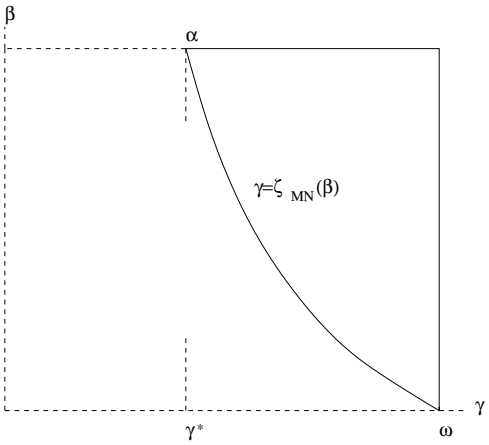

FIGURE 8. Schematic representation of the (γ, β)-plane for $M \leq N$ showing $Z_{MN} = 0$.

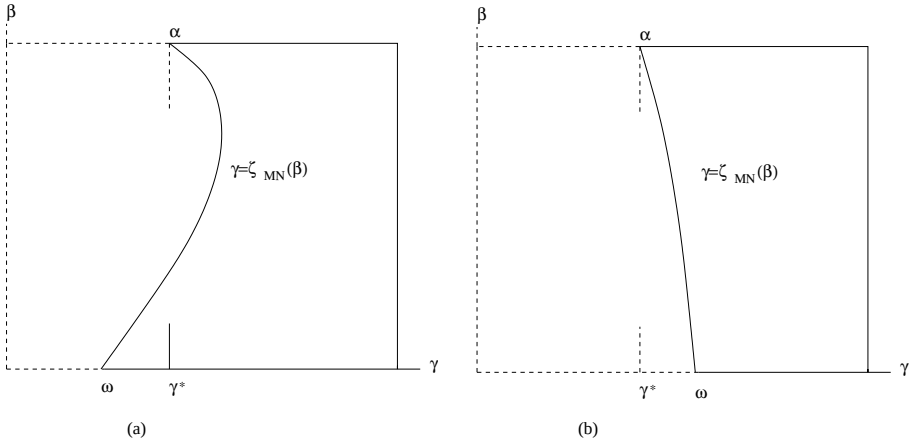

FIGURE 9. Schematic representation of the (γ, β)-plane for $N_a < M < N$ showing $Z_{MN} = 0$. There are two cases: (a) if $\gamma_{MN} < \gamma^*$ then the curve $\gamma = \zeta_{MN}(\beta)$ lies to the left of the line $\gamma = \gamma^*$ for all sufficiently small $\beta \geq 0$ and to the right of it for all sufficiently large values of β. (b) if $\gamma_{MN} > \gamma^*$ then the curve $\gamma = \zeta_{MN}(\beta)$ lies to the right of the line $\gamma = \gamma^*$ for all sufficiently small $\beta \geq 0$ and for all sufficiently large values of β.

roots. In fact our numerical studies show that there are no roots in this case. On the other hand, for $M > N_a + 1$, it follows from (26) that $X_{MN}(\gamma, 0) < 0$ between $\alpha = (\gamma_{M-1,N}, 0)$ and $\omega = (0, \infty)$. In particular, there is a least positive root $\beta = \xi_{M-1,N}(\gamma)$ whose graph joins α to ω. Again our numerical studies indicate that this graph is a smooth curve joining α to ω as shown in Figure 11.

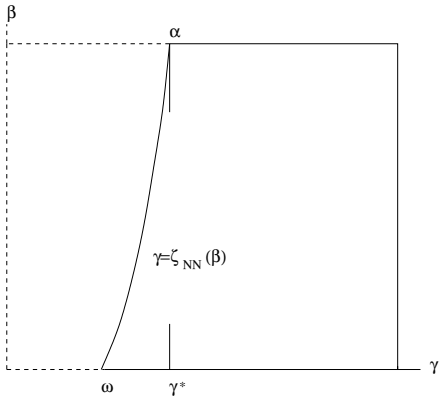

FIGURE 10. Schematic representation of the (γ, β)-plane for $M = N$ showing $Z_{NN} = 0$.

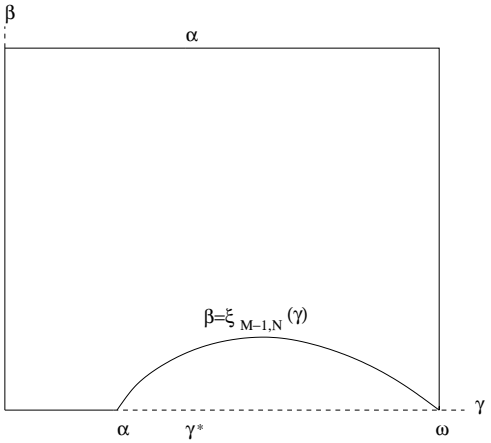

FIGURE 11. Schematic of the (γ, β) plane for $M > N_a + 1$, showing $X_{MN} = 0$.

To summarize:

- If $N_a + 1 < M \leq N$ then there is a standing wave solution which crosses threshold in G_M for every point (β, γ) between the curves $X_{MN}(\beta, \gamma) = 0$ and $Z_{MN}(\beta, \gamma) = 0$.
- If $N_a < M < N_a + 1$ then $\gamma_{MN} < +\infty$ and there is a standing wave solution which crosses threshold in G_M for every point (β, γ) to the right of the curve $Z_{MN}(\beta, \gamma) = 0$.
- If $1 \leq M < N_a$ then $\gamma_{MN} = +\infty$ and there is a standing wave solution which crosses threshold in G_M for every point (β, γ) to the right of the curve $Z_{MN}(\beta, \gamma) = 0$.

Figure 7(a) shows the numerically computed curves $X_{MN} = 0$ and $Z_{MN} = 0$ for $N = 5$ gaps with $a = 0.45$. Here $N_a = 2.75$ so that $\gamma_{M5} < \infty$ only for $M = 3, 4$, and 5. Note that the picture changes when a is varied. E. g., if $a = 0.4$ then $\gamma_{M5} < \infty$ only for $M = 4$ and 5 so that there are no curves $X_{M5} = 0$ for $M \leq 4$ as shown in Figure 7(b).

6. **Monotonicity.** The initial slope $u^*_{MN}(\gamma,\beta)$ which yields a monotone standing wave solution crossing threshold in the M^{th} gap in an N gap configuration has certain monotonicity properties with respect to the indices M and N. Specifically, we have

$$u^*_{1N} > u^*_{2N} > \cdots > u^*_{NN} \tag{31}$$

and

$$u^*_{MN} > u^*_{MN+1}. \tag{32}$$

An immediate consequence of (31) and (32) is

$$u^*_{MN} > u^*_{M+1,N+1}. \tag{33}$$

According to (14) with $k = 1$

$$u^*_{MN} = \frac{g_{N-M}}{f_{N-1} + (1+\gamma)g_{N-1}}$$

and (31) is an immediate consequence of the monotonicity of the g_k with respect to the index (12). To prove (32) we use (14) with $k = M$ to write (32) in the form

$$\frac{g_{N-M}}{g_{M-1}(f_{N-M} + \gamma g_{N-M}) + f_{M-1}g_{N-M}} > \frac{g_{N+1-M}}{g_{M-1}(f_{N+1-M} + \gamma g_{N+1-M}) + f_{M-1}g_{N+1-M}}.$$

Thus (32) is equivalent to

$$Q_{MN} \equiv g_{N-M}f_{N+1-M} - g_{N+1-M}f_{N-M} > 0. \tag{34}$$

If we write

$$(AP)^{N-M} = \begin{pmatrix} a_{11} & a_{12} \\ a_{21} & a_{22} \end{pmatrix}$$

then

$$f_{N-M} = a_{11} + a_{12} \text{ and } g_{N-M} = a_{21} + a_{22}.$$

Note that the $a_{ij} > 0$. Since

$$(AP)^{N-M+1} = \begin{pmatrix} a_{11}\cosh\beta + a_{12}\sinh\beta & a_{11}(\sinh\beta + \gamma\cosh\beta) + a_{12}(\cosh\beta + \gamma\sinh\beta) \\ a_{21}\cosh\beta + a_{22}\sinh\beta & a_{21}(\sinh\beta + \gamma\cosh\beta) + a_{22}(\cosh\beta + \gamma\sinh\beta) \end{pmatrix}$$

it follows that

$$f_{N-M+1} = a_{11}(\sinh\beta + (1+\gamma)\cosh\beta) + a_{12}(\cosh\beta + (1+\gamma)\sinh\beta)$$

and

$$g_{N-M+1} = a_{21}(\sinh\beta + (1+\gamma)\cosh\beta) + a_{22}(\cosh\beta + (1+\gamma)\sinh\beta).$$

Substituting in (34) yields

$$Q_{MN} = \gamma(\cosh\beta - \sinh\beta)\det\left\{(AP)^{N-M}\right\}.$$

However

$$\det\left\{(AP)^{N-M}\right\} = \{\det AP\}^{N-M}$$

and

$$\det AP = \begin{vmatrix} \cosh\beta & \sinh\beta + \gamma\cosh\beta \\ \sinh\beta & \cosh\beta + \gamma\sinh\beta \end{vmatrix} = \cosh^2\beta - \sinh^2\beta = 1.$$

Therefore

$$Q_{MN} = \gamma(\cosh\beta - \sinh\beta) > 0.$$

In Figure 7 the curves $Z_{MN} = 0$ lie to the right of the curves $Z_{M+1,N} = 0$. We show here that this monotonicity is a general property. In particular, we show that

$$Z_{MN}(\gamma,\beta) \geq 0 \text{ implies } Z_{M+1,N}(\gamma,\beta) > 0 \tag{35}$$

whenever both are defined. Using (15) we can write the condition $Z_{MN} \geq 0$ in the form

$$f_{N-1} + (1+\gamma)g_{N-1} \geq \frac{1}{a} f_{N-M} g_{M-1}. \tag{36}$$

Similarly

$$Z_{M+1,N} = f_{N-1} + (1+\gamma)g_{N-1} - \frac{1}{a} f_{N-M-1} g_M$$

so that (36) implies that

$$Z_{M+1,N} \geq \frac{1}{a} \left(f_{N-M} g_{M-1} - f_{N-M-1} g_M \right).$$

Therefore the sign of $Z_{M+1,N}$ is determined by the sign of

$$Q_{M+1,N} \equiv f_{N-M} g_{M-1} - f_{N-M-1} g_M.$$

By (11)

$$Q_{M+1,N} = \epsilon_1^T (AP)^{N-M} \epsilon \epsilon_2^T (AP)^{M-1} \epsilon - \epsilon_1^T (AP)^{N-M-1} \epsilon \epsilon_2^T (AP)^M \epsilon$$

which we rewrite as

$$Q_{M+1,N} = \epsilon_1^T (AP)^{N-M-1} R \, (AP)^{M-1} \epsilon,$$

where

$$R = AP \epsilon \epsilon_2^T - \epsilon \epsilon_2^T AP = \begin{pmatrix} -\sinh\beta & \sinh\beta + \gamma(\cosh\beta - \sinh\beta \\ -\sinh\beta & \sinh\beta \end{pmatrix}.$$

It is not difficult to verify that

$$APRAP = R. \tag{37}$$

Suppose first that $M \leq N/2$. Then it follows from (37) that

$$Q_{M+1,N} = \epsilon_1^T (AP)^{N-2M} R \epsilon = \gamma(\cosh\beta - \sinh\beta) a_{11} > 0,$$

where $(AP)^{N-2M} = (a_{ij})$ and all of the a_{ij} are positive..

If $M > N/2$ we have

$$Q_{M+!,N} = \epsilon_1^T R (AP)^{2M-N} \epsilon,$$

which, in view of (37), we rewrite as

$$Q_{M+1,N} = \epsilon_1^T \{(AP)^{2M-N}\}^{-1} R \epsilon. \tag{38}$$

Let $(AP)^{2M-N} = (b_{ij})$, where all of the b_{ij} are positive. Therefore, since $\det (AP)^{2M-N} = 1$ and

$$(AP)^{-1} = \begin{pmatrix} b_{22} & -b_{21} \\ -b_{12} & b_{11} \end{pmatrix},$$

it follows from (38) that

$$Q_{M+1,N} = \gamma(\cosh\beta - \sinh\beta) b_{22} > 0.$$

This completes the proof of (35).

In a similar manner we can show that

$$X_{MN}(\gamma,\beta) \geq 0 \text{ implies that } X_{M-1,N}(\gamma,\beta) > 0.$$

We omit the details.

7. **Solution crossing threshold in an active region.** We now consider the construction of monotone standing wave solutions which cross threshold in the M^{th} active region in an N gap configuration, where $M \in \{1, 2, ..., N-1\}$. This construction is considerably more complicated than the corresponding construction for solutions which cross threshold in a gap since now we have to deal explicitly with the nonlinearity of the problem.

To construct a standing wave solution which crosses threshold in the M^{th} active region A_M, we fix a $\delta \in [0,1]$, integrate the super-threshold equation $u'' - u + 1 = 0$ a distance $\delta\beta$ until u reaches the value a, and then integrate the sub-threshold equation $u'' - u = 0$ a distance $\beta(1-\delta)$ to complete the traversal of A_M. This is, of course, not possible for every choice of γ, β, and δ, but we will derive the admissible (γ, β)-set for any given δ. We will use the notation and conventions of Sections 3 and 4 .

If the initial slope is $-v^*$, then at the end of the gap G_M we have

$$U_{M-1} = \epsilon_1 - v^* P(AP)^{M-1}\epsilon,$$

where $A = A(\beta)$ and $P = P(\gamma)$. Assuming that the point U_{M-1} lies between the stable manifold Σ_2 and the line $u = a$, follow the trajectory of $u'' - u + 1 = 0$ for a distance $\delta\beta$ to obtain

$$\begin{pmatrix} a \\ u' \end{pmatrix} = \epsilon_1 - v^* A(\delta\beta) P(AP)^{M-1}\epsilon. \tag{39}$$

In particular, γ, β, δ, and v^* are constrained by the condition

$$a = 1 - v^* \epsilon_1^T A(\delta\beta) P(AP)^{M-1}\epsilon. \tag{40}$$

In addition, δ is constrained by the condition

$$0 \le \delta \le 1. \tag{41}$$

Continue by integrating the sub-threshold equation $u'' - u = 0$ for a distance $\beta(1-\delta)$ to obtain

$$V_M = A((1-\delta)\beta)\epsilon_1 - v^* A((1-\delta)\beta) A(\delta\beta) P(AP)^{M-1}\epsilon.$$

Finally proceeding as in Section 3, we arrive at

$$0 = \epsilon^T (PA)^{N-M-1} PA((1-\delta)\beta)\epsilon_1 \tag{42}$$
$$-v^* \epsilon^T P(AP)^{N-M-1} A((1-\delta)\beta) A(\delta\beta) P(AP)^{M-1}\epsilon.$$

(40) and (42) yield two expressions for the critical slope $-v^*$, and since they must agree we led to the condition

$$V_{MN}(\gamma, \beta; \delta) \equiv (1-a)\left\{\epsilon^T (PA)^{N-M-1} PA((1-\delta)\beta) A(\delta\beta) P(AP)^{M-1}\epsilon\right\} -$$
$$\left\{\epsilon^T (PA)^{N-M-1} PA((1-\delta)\beta)\epsilon_1\right\}\left\{\epsilon_1^T A(\delta\beta) P(AP)^{M-1}\epsilon\right\} = 0$$

for the existence of a heteroclinic orbit which crosses threshold in the M^{th} active region. Since $A(0) = I$,

$$V_{MN}(\gamma, \beta; 0) = -aZ_{MN}(\gamma, \beta)$$

and

$$V_{MN}(\gamma, \beta; 1) = -aX_{M+1,N}(\gamma, b),$$

where $X_{M+1,N}$ and Z_{MN} are defined in Section 4.

For each fixed $\delta \in [0,1]$ we can compute the set $V_{MN}(\gamma,\beta;\delta)=0$ in the (γ,β)-plane. Several examples are shown in Figure 12. If

$$1 \le M \le N_a \equiv (1-a)N$$

then for each

$$\delta \in [0,a)$$

the set $V_{MN}(\gamma,\beta;\delta)=0$ is a smooth curve in the (γ,β)-plane of the form $\gamma=\Gamma(\beta;\delta)$ with asymptotes at $\beta=0$ and $\beta=\beta^*(\delta)$, where β^* is the unique positive solution to

$$\tanh((1-\delta)\beta)\tanh(\delta\beta)=\frac{a-\delta}{1-a-\delta}. \tag{43}$$

These curves fill out the region in the (γ,β)-plane to the right of $Z_{MN}(\gamma,\beta)=-\frac{1}{a}V_{MN}(\gamma,\beta;0)=0$. The set $V_{MN}(\gamma,\beta;\delta)=0$ is empty for $\delta \ge a$. An example is given in Figure 12(a).

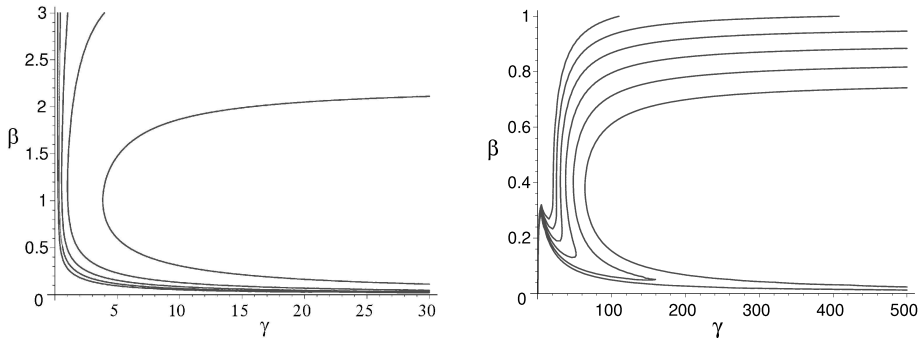

FIGURE 12. The (γ,β)-plane for the three-gap problem with $a=0.45$. (a) The curves $V_{13}(\gamma,\beta;\delta)=0$ are shown (from left to right) for $\delta=0,0.1,...,0.4$. Here $N_a=1.65>M=1$. (b) The curves $V_{33}(\gamma,\beta;\delta)=0$ are shown (from left to right) for $\delta=0.440,0.441,...,0.445$. Here $N_a+1=2.65<M=3$. Note that for the range of γ in this figure $V_{33}(\gamma,\beta;0.445)=0$ shows two components.

The formula (43) is derived by considering the asymptotic behavior of V_{MN} for $\gamma \gg 1$. Observe that

$$(PA)^{N-M-1} \sim \gamma^{N-M-1}(\sinh(\beta))^{N-M-2}\begin{pmatrix}\sinh(\beta) & \cosh(\beta)\\ 0 & 0\end{pmatrix},$$

$$(AP)^{M-1} \sim \gamma^{M-1}(\sinh(\beta))^{M-2}\begin{pmatrix}0 & \cosh(\beta)\\ 0 & \sinh(\beta)\end{pmatrix},$$

and

$$P \sim \gamma\begin{pmatrix}0 & 1\\ 0 & 0\end{pmatrix}$$

as $\gamma \to \infty$. Therefore

$$V_{MN}(\gamma,\beta;\delta) \sim \gamma^N(\sinh(l))^{N-2}\{(1-a)\cosh((1-\delta)\beta)\sinh(\delta\beta) \tag{44}$$
$$-a\sinh((1-\delta)\beta)\cosh(\delta\beta)\}$$

as $\gamma \to \infty$. It follows from (44) that $V_{MN} \sim 0$ as $\gamma \to \infty$ if either $\gamma^N(\sinh(l))^{N-2} \to 0$ as $\gamma \to \infty$ or (43) has a solution $\beta=\beta^*>0$.

For

$$N_a < M \leq N$$

the situation is somewhat different because in addition to the curve $Z_{MN} = 0$ there is also the curve $X_{M+1,N} = 0$, and the sets $V_{MN} = 0$ fill out the region between them. For each

$$\delta \in [a, 1]$$

the set $V_{MN}(\gamma, \beta; \delta) = 0$ is a curve starting at $(\gamma_{MN}, 0)$ and approximating $X_{M+1,N}(\gamma, \beta) = 0$ as $\gamma \to \infty$. For each

$$\delta \in (0, a)$$

the set $V_{MN}(\gamma, \beta; \delta) = 0$ is a curve starting at $(\gamma_{MN}, 0)$ which asymptotes at $\beta = \beta^*(\delta)$ for $\gamma \to \infty$. For δ very close to a this curve stays close to $X_{M+1,N} = 0$ for very large value of γ before switching to it's asymptotic behavior. An example is given in Figure 12 (b). (Our numerical evidence is not sufficiently sharp to rule out the possibility that for δ near a the set $V_{MN} = 0$ possesses two components; one which approximates $X_{M+1,N} = 0$ and another which asymptotes at $\beta = 0$ and $\beta = \beta^*$.)

We can also use (40) and (41) to study the relationship between the active region length β and the critical initial slope $-v^*$. Using (11) and the fact that $\cosh(l)^2 - \sinh(l)^2 = 1$ we rewrite (40) in the form

$$\frac{1-a}{v} - g_{M-1}\sinh(\delta\beta) = (f_{M-1} + \gamma g_{M-1})\sqrt{1 + \sinh(\delta\beta)^2},$$

where we have written v in place of v^*. This is a quadratic equation for $\sinh(\delta\beta)$ which we solve to obtain

$$\delta^*(\gamma, \beta, v) \equiv \frac{1}{\beta}\arcsin h\left\{\frac{-(1-a)g_{M-1} + (f_{M-1} + \gamma g_{M-1})\sqrt{(1-a)^2 - v^2 p_{M-1}}}{v p_{M-1}}\right\},$$

where

$$p_{M-1} = p_{M-1}(\gamma, \beta) \equiv (f_{M-1}(\gamma, \beta) + \gamma g_{M-1}(\gamma, \beta))^2 - g_{M-1}(\gamma, \beta)^2.$$

In view of the constraint (41) we define

$$\delta = \delta(\gamma, \beta, v) \equiv \begin{cases} 0 \text{ if } \delta^*(\gamma, \beta, v) < 0 \\ \delta^*(\gamma, \beta, v) \text{ if } 0 \leq \delta^*(\gamma, \beta, v) \leq 1 \\ 1 \text{ if } \delta^*(\gamma, \beta, v) > 1 \end{cases} . \tag{45}$$

Using the formula (45) in (42) we obtain a relationship between γ, β, and the critical initial slope $-v$. For each fixed γ this is an implicit relationship between v and the active region length β , and we can plot the resulting curves in the (v, β)-plane. Figures 3 and 5 show the results of this computation for a two-gap configuration. Figure 13 shows some results for the case of three gaps. Note that by using (45) we account for threshold crossings not only in A_M, but also in G_M when $\delta = 0$ and in G_{M+1} when $\delta = 1$. Thus the curves which we generate in this manner show the bifurcations which occur when the threshold is crossed at the intersection of an active and a passive region.

There remains to be considered the case in which the standing wave solution crosses threshold in the terminal active region A_N. At the end of the N^{th} gap G_N, since threshold has not yet been crossed, we have

$$U_{N-1} = \epsilon_1 - uP(AP)^{N-1}\epsilon. \tag{46}$$

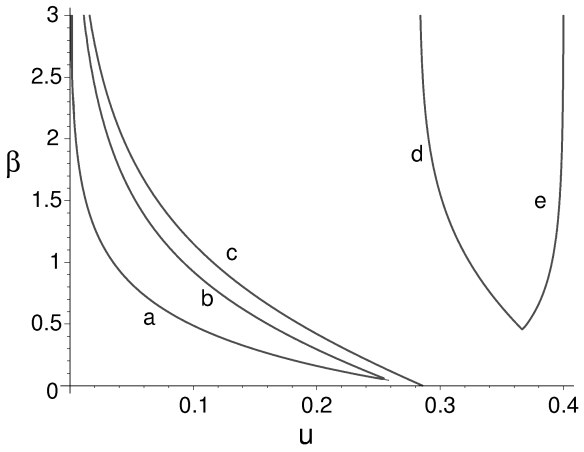

FIGURE 13. The (u, β)-plane for the three-gap problem with threshold $a = 0.45$ and gap length $\gamma = 0.5$. Here $-u$ is the initial slope and β is the length of the intervals in the active region. For points (u, β) on the curves labeled a, c, e the corresponding standing wave solution crosses threshold in the gaps G_1, G_2, G_3 respectively. For points on the curves labeled b, d the corresponding standing wave solutions cross threshold in the active regions A_2, A_1 respectively. There are two bifurcation points: one at the intersection of the curves a and b, and the other at the intersection of the curves d and e.

We require that this point lies on the right-most branch

$$\Sigma_2 : (u-1)^2 - u'^2 = 1 - 2a \quad \text{for} \quad -a \le u' \le 0 \tag{47}$$

of the stable manifold of $(0, 0)$. Substituting from (46) in (47) yields

$$v_{N+1}^{*2} \left\{ (f_{N-1} + \gamma g_{N-1})^2 - g_{N-1}^2 \right\} = 1 - 2a.$$

To satisfy the condition $u' \ge -a$ we must have

$$v_{N+1,M}^* \le \frac{a}{g_{N-1}}$$

which reduces to

$$a^2 (f_{N-1} + \gamma g_{N-1})^2 - (1-a)^2 g_{N-1,M}^2 \ge 0.$$

Thus, in particular, the condition for the existence of a heteroclinic orbit which crosses threshold in the terminal active region A_M is

$$a(f_{N-1} + \gamma g_{N-1}) - (1-a) g_{N-1} = a Z_{NN}(\gamma, \beta) \ge 0.$$

8. **Stability.** We now investigate the stability properties of the standing wave solutions which we have constructed. In particular, we prove that the standing waves which cross threshold in a gap are stable, while those which cross in an active region are unstable. If threshold is crossed at the intersection of a gap and an active region, then there is one-sided stability. The proofs of these results are based on an extension to discontinuous parabolic operators of the standard comparison principle and the stabilization theorem of Aronson&Weinberger [1, 2]. In order to apply these results we will construct suitable stationary sub- and super-solutions in neighborhoods of our monotone standing waves.

We are concerned with the parabolic differential operator

$$\mathcal{N}u \equiv u_t - u_{xx} - I(x)\left\{H(u-a) - u\right\},$$

where $I(x)$ is the indicator function on the union of the active regions. $\mathcal{N}$ is discontinuous at the intersections of the active and passive regions as well as on any curve $x = c(t)$ where $u(c(t), t) = a$. We will assume, in general, that $\mathcal{N}$ is discontinuous on a finite collection of curves $\mathcal{C} = \{c_1(t), ..., c_m(t)\}$ which are nowhere horizontal.

Comparison Theorem. *Let $\varphi(x,t) = u(x,t) - v(x,t)$, where u and v are $C^{2,1}((\mathbf{R}\backslash\mathcal{C}) \times \mathbf{R}^+) \cap C(\mathbf{R} \times \mathbf{R}^+)$ functions. If*

$$\begin{aligned} \mathcal{N}\varphi &\leq 0 \text{ in } (\mathbf{R}\backslash\mathcal{C}) \times \mathbf{R}^+ \\ \varphi(\cdot, 0) &\leq 0 \text{ in } \mathbf{R} \\ \varphi_x(c_j(t)-, t) &\leq \varphi_x(c_j(t)+, t) \quad \text{for } j = 1, ..., m \quad \text{and } t \in \mathbf{R}^+. \end{aligned}$$

then

$$\varphi(x,t) \leq 0 \text{ throughout } \mathbf{R} \times \mathbf{R}^+.$$

An important consequence of the Comparison Theorem concerns the behavior of solutions to the transient problem when the initial datum is a stationary sub- or super-solution. A function U is said to be a *sub-solution* for $\mathcal{N}$ if

$$\mathcal{N}U \leq 0 \text{ in } (\mathbf{R}\backslash\mathcal{C}) \times \mathbf{R}^+ \tag{48}$$

$$U_x(c_j(t)-, t) \leq U_x(c_j(t)+, t) \text{ for } j = 1, ..., m \text{ and } t \in \mathbf{R}^+,$$

and U is said to be a *super-solution* for $\mathcal{N}$ if (48) holds with the inequalities reversed. If U is a sub-solution and v is a solution with $U(\cdot, 0) \leq v(\cdot, 0)$ then, according to the Comparison Theorem, $U(x,t) \leq v(x,t)$ everywhere. Moreover, we have the next theorem.

Convergence Theorem. *Let $U(x)$ be a time-independent sub-solution (super-solution) for $\mathcal{N}$ and let $u(x,t;U)$ be the solution of the transient problem*

$$\begin{aligned} \mathcal{N}u &= 0 \quad \text{in } (\mathbf{R}\backslash\mathcal{C}) \times \mathbf{R}^+ \\ u(\cdot, 0) &= U \quad \text{in } \mathbf{R}. \end{aligned}$$

Then $u(x,t;U)$ is a nondecreasing (nonincreasing) function of t which for $t \to \infty$ approaches the smallest (largest) steady state solution $U^*(x)$ of $\mathcal{N}u = 0$ such that

$$U^*(x) \geq (\leq) U(x) \text{ for all } x \in \mathbf{R}.$$

Proofs of these results are essentially given by Pauwelussen [12]. In order to apply these results we prove the existence of suitable sub- and super-solutions in the neighborhood of each standing wave solution. In particular, we show that a standing wave solution which crosses threshold in a gap is stable since there exist sub-solutions below and super-solutions above it. For a standing wave solution $W(x)$ which crosses threshold in an active region the situation is more complicated since the transition from super- to sub-threshold reverses relative positions. Thus the sub- and super-solutions which we construct straddle the standing wave rather than being strictly above or below it. Suppose W crosses threshold in the M^{th} active region. We construct steady super-solutions W^+ and sub-solutions W^- arbitrarily close to W which satisfy $W^+ < W < W^-$ on $(0, x_M)$. By the Convergence Theorem $u(x,t;W^+)$ $(u(x,t;W^-))$ converges to the largest (smallest) steady state solution S satisfying $S < W$ $(S > W)$. Thus W is unstable.

Moreover, if we consider a transient problem whose initial datum lies between two standing waves, one crossing threshold in A_{M-1} and the other crossing in A_M, then it follows from the Comparison Theorem and the Convergence Theorm that the solution to that problem will evolve in time to a standing wave which crosses threshold in G_M. This is illustrated in Figure 14.

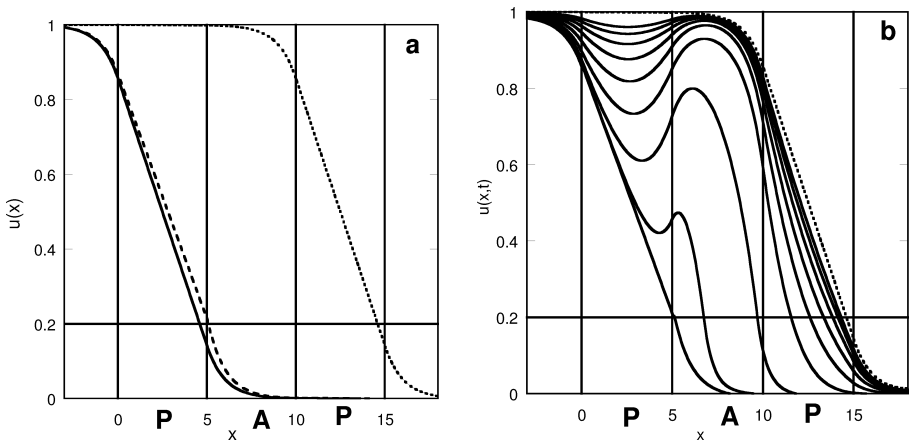

FIGURE 14. (a) The three standing wave solutions corresponding to the two-gap case ($a = 0.2, \beta = \gamma = 5.$). Solid, dashed and dotted lines represent the standing wave for which the solution crosses threshold within the first gap, the first active region, and the second gap, respectively. (b) Transient simulation for initial condition: $u_0(x) = u_{sw}(x) + \epsilon$, where $u_{sw}(x)$ is the standing wave for which the solution drops below threshold within the first active region in (a) and $\epsilon = -0.01$. The final distribution is shown in a dotted line and is identical to the constructed standing wave shown in (a).

The standing wave which crosses threshold in the M^{th} gap for a specific (γ, β) is given by (16), where u^*_{MN} is the initial speed determined by the condition that the endpoint of the phase curve for the standing wave lies on the stable manifold Σ_1. If we omit this condition and write (16) for arbitrary values of u, then it is clear that both $u(x)$ and $u'(x)$ decreases as u increases. If $u_1 < u^*_{MN} < u_2$, let

$$U_{N-1}(u_j) = \begin{pmatrix} U_j \\ U'_j \end{pmatrix} \text{ and } U_{N-1}(u^*_{MN}) = \begin{pmatrix} U_* \\ U'_* \end{pmatrix}$$

then

$$\begin{aligned} U_1 &> U_* > U_2, \\ U'_1 &> U'_* > U'_2 \end{aligned}$$

and

$$q_1 > 0 > q_2,$$

where $q_j = U_j + U'_j$ with $U_* + U'_* = 0$ by construction. It follows that the phase point (U_1, U'_1) lies above Σ_1 while the point (U_2, U'_2) lies below it, as shown in Figure 15. We construct a sub-solution below the standing wave by introducing an upward jump in the derivative at $x = y_{N-1}$ by setting

$$U'_2(y_{N-1}+) = -U_2 > U'_2(y_{N-1}-).$$

Similarly, we construct a super-solution above the standing wave by introducing a

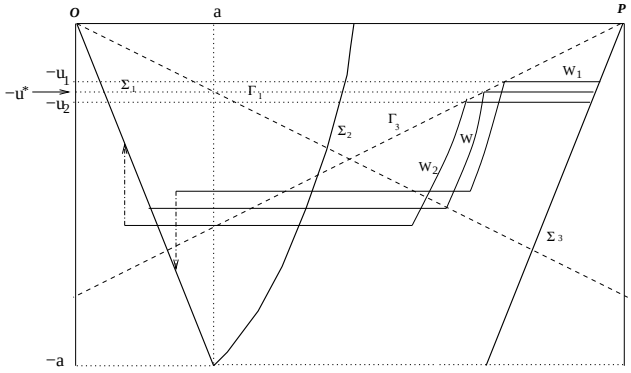

FIGURE 15. Construction of sub- and super- solutions close to a standing wave W which crosses threshold in the gap G_2 in the two-gap problem. W_1 is a super-solution which lies above W and W_2 is a sub-solution that lies below W.

downward jump in derivative at $x = y_{N-1}$ by setting

$$U_1'(y_{N-1}+) = -U_1 < U_1'(y_{N-1}-).$$

Suppose now that threshold is reached in the M^{th} active region A_M at $\overline{y} = x_M+\delta$, where $\delta \in (0, \beta)$. Then

$$\begin{pmatrix} a \\ u'(\overline{y}) \end{pmatrix} = \epsilon_1 - uA(\delta)P(AP)^{M-1}\epsilon$$

and $\delta = \delta(u)$ is determined by

$$a = 1 - u\epsilon_1^T A(\delta)P(AP)^{M-1}\epsilon.$$

Differentiating with respect to u and using the fact that

$$\frac{d}{d\delta}A(\delta) = \begin{pmatrix} 0 & 1 \\ 1 & 0 \end{pmatrix} A(\delta)$$

yields

$$\frac{d\delta}{du} = -\frac{\epsilon_1^T A(\delta)P(AP)^{M-1}\epsilon}{u\epsilon_2^T A(\delta)P(AP)^{M-1}\epsilon} < 0. \tag{49}$$

Set $b(u) = u'(x_M + \delta(u))$. Then

$$b(u) = -u\epsilon_2^T A(\delta)P(AP)^{M-1}\epsilon$$

and

$$\frac{db}{du} = -\epsilon_2^T A(\delta)P(AP)^{M-1}\epsilon - u\frac{d\delta}{du}\epsilon_1^T A(\delta)P(AP)^{M-1}\epsilon.$$

In view of (49) this becomes

$$\frac{db}{du} = \frac{\left\{\epsilon_1^T A(\delta)P(AP)^{M-1}\epsilon\right\}^2 - \left\{\epsilon_2^T A(\delta)P(AP)^{M-1}\epsilon\right\}^2}{\epsilon_2^T A(\delta)P(AP)^{M-1}\epsilon}.$$

The sign of db/du is determined by the sign of

$$(\epsilon_1^T - \epsilon_2^T)A(\delta)P(AP)^{M-1}\epsilon = (\cosh(\beta) - \sinh(\beta))(f_{M-1} - g_{M-1} + \gamma g_{M-1}).$$

Therefore

$$\frac{db}{du} > 0. \tag{50}$$

To complete the traversal of A_M we apply $A(\beta - \delta)$ to obtain

$$\begin{pmatrix} v_M(u) \\ v'_M(u) \end{pmatrix} = A(\beta - \delta(u)) \begin{pmatrix} a \\ b(u) \end{pmatrix}$$

Suppose $0 < u_1 < u_* = v^*_{MN} < u_2$. Then

$$\begin{pmatrix} v_M(u_1) \\ v'_M(u_1) \end{pmatrix} = \begin{pmatrix} a\cosh(\beta - \delta(u_1)) + b(u_1)\sinh(\beta - \delta(u_1)) \\ a\sinh(\beta - \delta(u_1)) + b(u_1)\cosh(\beta - \delta(u_1)) \end{pmatrix}$$

and by Taylor's expansion

$$\begin{pmatrix} v_M(u_1) \\ v'_M(u_1) \end{pmatrix} = \begin{pmatrix} v_M(u_*) \\ v'_M(u_*) \end{pmatrix} + (u_* - u_1)R + \cdots,$$

where

$$R = \begin{pmatrix} \delta'(u_*)\{a\sinh(\beta - \delta(u_*)) + b(u_*)\cosh(\beta - \delta(u_*))\} - b'(u_*)\sinh(\beta - \delta(u_*)) \\ \delta'(u_*)\{a\cosh(\beta - \delta(u_*)) + b(u_*)\sinh(\beta - \delta(u_*))\} - b'(u_*)\cosh(\beta - \delta(u_*)) \end{pmatrix}.$$

In view of (49) and (50), both components of R are negative, so that

$$v_M(u_1) < v_M(u_*) \text{ and } v'_M(u_1) < v'_M(u_*) \tag{51}$$

for sufficiently large $u_1 < u_*$. Similarly

$$v_M(u_2) > v_M(u_*) \text{ and } v'_M(u_2) > v'_M(u_*) \tag{52}$$

for sufficiently small $u_2 > u_*$.

At the end of the last gap G_N we have

$$U_{N-1}(u) = \begin{pmatrix} u_{N-1}(u) \\ u'_{N-1}(u) \end{pmatrix} = P(AP)^{N-M-1} \begin{pmatrix} v_M(u) \\ v'_M(u) \end{pmatrix}.$$

The elements of the matrix $P(AP)^{N-M-1}$ are all strictly positive and independent of u. Therefore it follows from (51 and (52) that

$$u_{N-1}(u_1) < u_{N-1}(u_*) \text{ and } u'_{N-1}(u_1) < u'_{N-1}(u_*)$$

and

$$u_{N-1}(u_2) > u_{N-1}(u_*) \text{ and } u'_{N-1}(u_2) > u'_{N-1}(u_*).$$

Moreover

$$q(u_1) < q(u_*) = 0 < q(u_2).$$

Thus the phase point $U_{N-1}(u_1)$ is in the fourth quadrant below Σ_1 and the phase point $U_{N-1}(u_2)$ is in the fourth quadrant above Σ_1 provided that u_1 and u_2 are sufficiently close to u_* with $u_1 < u_* < u_2$.

Let $W(x;u)$ denote the steady state solution so far constructed for $x \in (-\infty, x_N)$, where $W(x;u_*)$ is the standing wave solution which crosses threshold in A_M. We extend the domain of $W_1(x) = W(x;u_1)$ by setting

$$W'_1(x_N+) = -W_1(x_N) > W'_1(x_N-)$$

and continuing the integration along the stable manifold Σ_1. Thus $W_1(x)$ is a steady sub-solution for the operator $\mathcal{N}$. According to the Convergence Theorem, $u(x.t;W_1)$ converges with $t \to \infty$ to the smallest steady state solution S such that $W_1(x) \le S(x)$. Since $u_1 < u_*$ we have

$$W_1(x) > W(x;u_*) \text{ for } x \in (0, \in x_M)$$

and it follows that

$$W(x;u_*) < S(x) \text{ for all } x.$$

In a similar manner if we extend W_2 by setting

$$W_2'(x_N+) = -W_2(x_N) < W_2'(x_N-)$$

then $W_2(x)$ is a steady super-solution, and $u(x,t;W_2)$ converges down as $t \to \infty$ to the largest steady state solution $T(x)$ such that

$$W(x;u_*) > T(x) \text{ for all } x$$

(cf. Figure 16).

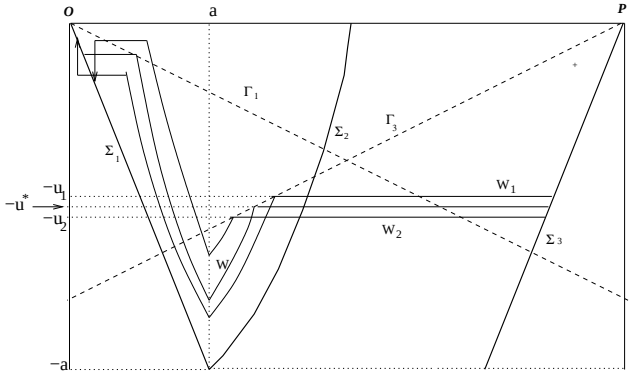

FIGURE 16. Construction of sub- and super- solutions close to a standing wave W which crosses threshold in the active region A_1 in the two-gap problem. W_1 is a sub-solution which lies partially above W and W_2 is a super-solution which lies partially below W.

Bifurcations occur when threshold is crossed at the intersection of an active and a passive region. Suppose, for example, that the standing wave crosses threshold at the intersection of G_M and A_M. Then, as above, for $u_2 > u_*$ we can construct sub-solutions strictly below the standing wave, and for $u_1 < u_*$ sub-solutions which straddle the wave but which lie partially above it (cf. Figure 16). Thus the standing wave is stable from below and unstable from above. A crossing of threshold at the intersection of A_M and G_{M+1} can only occur for $M > N_a + 1$. The corresponding standing wave solution is stable from above and unstable from below.

To more fully delineate the domain where blockage can occur we need two more observations. The first is that any monotone standing wave solution which crosses threshold in the terminal active region A_N is unstable. The second is the existence of a "universal" sub-solution below any of the standing wave solutions. A transient solution whose initial datum lies below the unstable steady state wave which crosses in A_M and above the universal sub-solution will be blocked. If the initial datum lies above the unstable steady state the solution will propagate.

At the end of the N^{th} gap

$$U_{N-1}(u) = \begin{pmatrix} u_{N-1}(u) \\ u'_{N-1}(u) \end{pmatrix} = \begin{pmatrix} 1 - u\,(f_{N-1} + \gamma g_{N-1}) \\ u g_{N-1} \end{pmatrix}, \tag{53}$$

where

$$\begin{pmatrix} u_{N-1}(u_*) \\ u'_{N-1}(u_*) \end{pmatrix} \in \Sigma_2. \tag{54}$$

If $u_1 < u_* < u_2$ then

$$u_{N-1}(u_1) > u_{N-1}(u_*) > u_{N-1}(u_2) \text{ and } u'_{N-1}(u_1) > u'_{N-1}(u_*) > u'_{N-1}(u_2). \quad (55)$$

Let

$$q(w) \equiv (1 - u_{N-1}(w))^2 - u'^2_{N-1}(w),$$

where, in view of (54), $q(u_*) = 1 - 2a$ and, in view of (53),

$$q(u) = u^2 \left\{ (f_{N-1} + \gamma g_{N-1})^2 - g^2_{N-1} \right\}.$$

Note that

$$(f_{N-1} + \gamma g_{N-1})^2 - g^2_{N-1} = (f_{N-1} + \gamma g_{N-1} + g_{N-1})(f_{N-1} - g_{N-1} + \gamma g_{N-1}) > 0.$$

Therefore $q(u)$ is a strictly increasing function and

$$q(u_1) < q(u_*) = 1 - 2a < q(u_2).$$

Since $q(u_1) < 1 - 2a$ the phase point $U_{N-1}(u_1)$ lies between Σ_2 and Σ_3. We construct a sub-solution by setting

$$u'_{N-1}(u_1)\,|_{x_N+} = -\sqrt{\{(1 - u_{N-1}(u_1))^2 - 1 + 2a\}} > u'_{N-1}(u_1)\,|_{x_N-}\,.$$

In view of (55) this sub-solution lies above the standing wave. In a similar manner we can construct super-solutions below the standing wave. An example is shown in Figure 17. Thus any standing wave solution which crosses threshold in the terminal active region A_N is unstable.

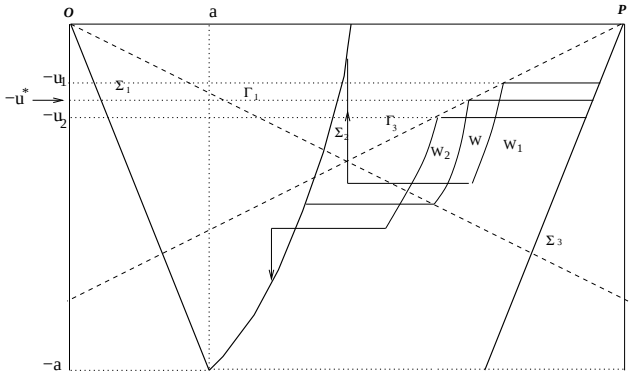

FIGURE 17. Construction of sub- and super- solutions close to a standing wave W which crosses threshold in the terminal active region A_2 in the two-gap problem. W_1 is a sub-solution which lies above W and W_2 is a super-solution which lies below W.

To construct the universal sub-solution we first consider the case $\gamma \geq \dfrac{1}{a} - 1$. The locus of endpoints of phase curves in the first passive region is the line $u = 1 + (1 + \gamma)u'$ which intersects the line $u = 0$ at or above the level $u' = -a$. This means that the phase curve reaches $u = 0$ before the end of the first gap. The sub-solution consists of the this phase curve cut off at $u = 0$ and continued as $u \equiv 0$ (cf. Figure 18(a)). For $\gamma^* < \gamma < \dfrac{1}{a} - 1$ the phase curve for the first gap reaches the level $u' = -a$ for some $u \in (0, a)$. Then integration is then continued into A_1 where depending on the magnitude of β it may reaches $u = 0$. If it does we continue it as

$u \equiv 0$. If not then we continue into G_2 where it must reach $u = 0$ (cf. Figures 18(b) and 18(c)).

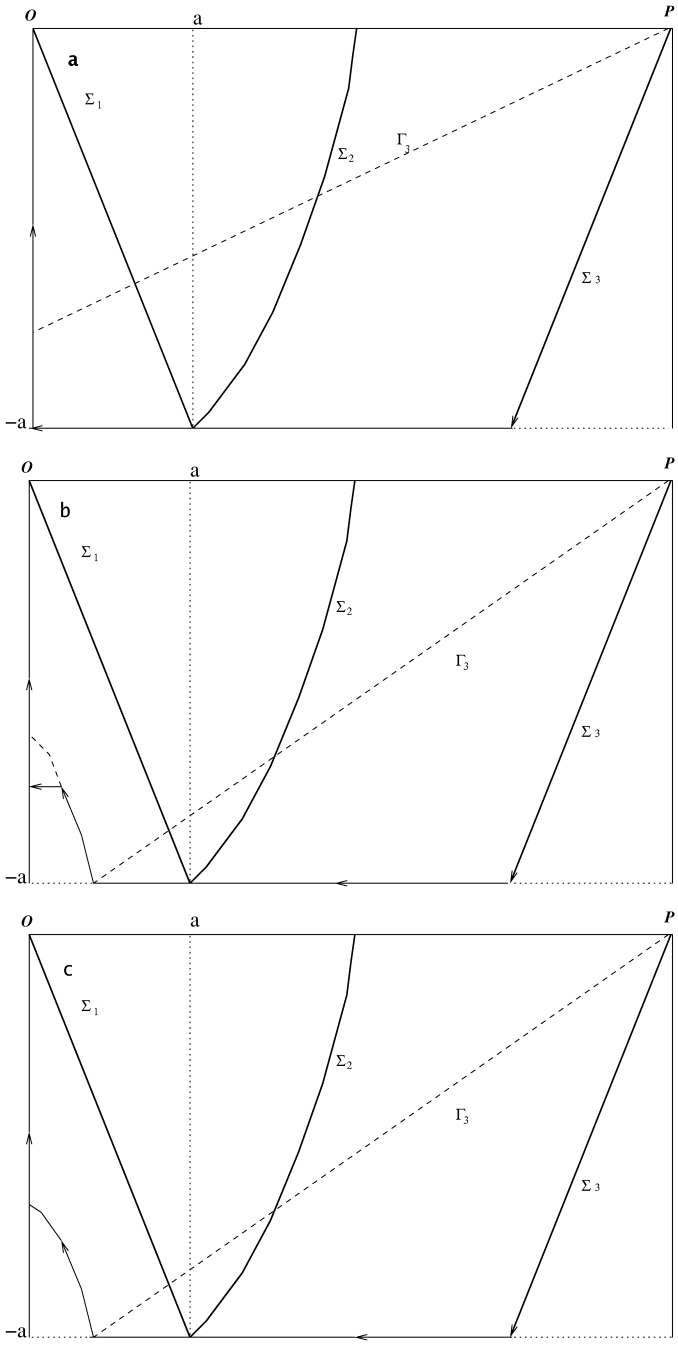

FIGURE 18. Construction of the "universal" sub-solution for (a) $\gamma \geq \frac{1}{a} - 1$, (b) and (c) $\gamma^* < \gamma < \frac{1}{a} - 1$.

9. **Discussion.** We have considered a problem of signal propagation in a non-homogeneous medium. Specifically, we consider the real line partitioned into a passive region $\mathfrak{P}$ consisting of N open intervals each of length γ, and an active region $\mathfrak{A}$ consisting of $N-1$ open intervals each of length β separating the intervals of $\mathfrak{P}$ together with two semi-infinite intervals surrounding $\mathfrak{P}$ (cf. Figure 1). We have studied the evolution of a quantity $u(x,t)$ that satisfies the diffusion equation

$$u_t = u_{xx}$$

for $x \in \mathfrak{P}$ and the McKean-Nagumo reaction-diffusion equation

$$u_t = u_{xx} + H(u-a) - u$$

for $x \in \mathfrak{A}$. If $\mathfrak{P} = \emptyset$ then, for all but a codimension-1 manifold of initial data, solutions to the initial value problem for the McKean-Nagumo equation approach either the stable equilibrium $u \equiv 0$ or $u \equiv 1$ as $t \to \infty$ [10]. If $\mathfrak{P} \neq \emptyset$ and γ is sufficiently small then the situation is similar to the case $\mathfrak{P} = \emptyset$, i.e., most solutions either die out (tend to 0) or propagate (tend to 1). However for appropriate values of γ and β in the first quadrant of the (γ,β)-plane (roughly speaking, for γ sufficiently large, cf. Figures 6 and 11) there exist stable and unstable standing wave solutions which induce a new class of asymptotics, namely, non-trivial stationary patterns. Thus for appropriate initial data the solution to the initial value problem does not tend asymptotically to one of the constant equilibria $u \equiv 0$ or $u \equiv 1$, but instead tends to one of the standing waves. In particular, for the standing waves $u \to 0$ as $x \to \infty$ so there is no transmission across the passive region $\mathfrak{P}$.

An interesting extension of the present work would be to systems of equations involving a recovery variable, e.g., the system

$$v_t = v_{xx} + I(x)\{H(v-a) - v - \varepsilon w\} \tag{56}$$

$$w_t = I(x)(bv - cw),$$

where $I(x)$ is the indicator function of the active regions, b and c are positive constants, and ε is a non-negative parameter. For $\varepsilon = 0$ the system (56) reduces to the McKean-Nagumo equation, while for $\varepsilon = 1$ and $I(x) \equiv 1$ the system (56) is the FitzHugh-Nagumo-McKean system studied by Rinzel & Keller [13] and others. Clearly for $\varepsilon > 0$ the presence of the recovery variable w will facilitate wave block. For $\varepsilon \ll 1$ one can analyze standing waves and pulses for (56) in the spirit of what we have done here for the McKean-Nagumo equation. There is however one major difference. In the single equation case we were able to use comparison methods to establish nonlinear stability and instability properties of standing wave solutions. Comparison methods are not, in general, applicable to systems such as (56) so that one usually has to settle for a linearized stability analysis. Nevertheless we conjecture that the McKean/Moll analysis of the gap-free case can be extended to the case in which there are gaps for sufficiently small ε. For $\varepsilon = 1$ there are various phenomena other than wave-block, e.g., wave reversal [14]. Thus it would be interesting to study the continuation of the solution set to (56) with respect to the parameter ε.

10. **Acknowledgments.** NVM and HGO were supported in part by NIH Grant # GM29123, and by the Minnesota Supercomputing Institute. NVM was also supported in part by NSF-BES # 0331324.

11. **Appendix.** *Proof of (28) , (29) and (30).* Write

$$AP = \frac{e^{\beta}}{2}R + \frac{e^{-\beta}}{2}S,$$

where

$$R = \begin{pmatrix} 1 & 1+\gamma \\ 1 & 1+\gamma \end{pmatrix} \text{ and } S = \begin{pmatrix} 1 & -1+\gamma \\ -1 & 1-\gamma \end{pmatrix},$$

and

$$AP = \frac{e^{\beta}}{2}U + \frac{e^{-\beta}}{2}V,$$

where

$$U = \begin{pmatrix} 1+\gamma & 1+\gamma \\ 1 & 1 \end{pmatrix} \text{ and } V = \begin{pmatrix} 1-\gamma & -1+\gamma \\ -1 & 1 \end{pmatrix}.$$

Note that for any positive integer k

$$R^k\epsilon = (2+\gamma)^{k-1}R\epsilon = (2+\gamma)^k\epsilon \tag{57}$$

and

$$\epsilon^T U^k = (2+\gamma)^{k-1}\epsilon^T U = (2+\gamma)^k\epsilon^T. \tag{58}$$

Then for $M \geq 2$

$$(AP)^{M-1}\epsilon = \frac{e^{(M-1)\beta}}{2^{M-1}}(2+\gamma)^{M-1}\epsilon + \frac{e^{(M-3)\beta}}{2^{M-1}}B_{M-1}\epsilon + \cdots,$$

where

$$B_{M-1} = \sum_{j=0}^{M-2} R^{M-2-j}SR^j\ ,$$

and for $M \leq N-1$

$$\epsilon^T(PA)^{N-M} = \frac{e^{(N-M)\beta}}{2^{N-M}}\epsilon^T(2+\gamma)^{N-M} + \frac{e^{(N-M-2)\beta}}{2^{M-1}}\epsilon^T D_{N-M} + \cdots,$$

where

$$D_{N-M} = \sum_{j=0}^{N-M-1} U^{N-M-1-j}VU^j.$$

If $M = 1$ then $B_0 = 0$ and $D_0 = 0$ when $M = N$.

Since

$$\begin{pmatrix} f_k(\gamma,\beta) \\ g_k(\gamma,\beta) \end{pmatrix} = (AP)^k\epsilon \sim (2+\gamma)^k\left(\frac{e^{\beta}}{2}\right)^k\epsilon \text{ as } \beta \to \infty.$$

it follows that

$$\begin{aligned} X_{MN} &= (\frac{1}{a}-1)g_{M-1}(f_{N-M}+\gamma g_{N-M}) - f_{M-1}g_{N-M} \\ &\sim (2+\gamma)^{N-1}\left(\gamma^* + \gamma(\frac{1}{a}-1)\right)\frac{e^{(N-1)\beta}}{2^{N-1}} \text{ as } \beta \to \infty. \end{aligned}$$

Thus (28) holds.

To prove (29) we note that in view of (11) and (13) we can write (21) in the form.

$$Z_{MN} = \epsilon^T(PA)^{N-M}Q(AP)^{M-1}\epsilon,$$

where

$$Q = \begin{pmatrix} 1 & \gamma \\ 0 & 1-\frac{1}{a} \end{pmatrix}.$$

Hence

$$\begin{aligned} Z_{MN} &= \frac{e^{(N-1)\beta}}{2^{N-1}}(2+\gamma)^{N-1}\epsilon^T Q\epsilon \\ &\quad + \frac{e^{(N-3)\beta}}{2^{N-1}}\{(2+\gamma)^{N-M}\delta\epsilon^T QB_{M-1}\epsilon + (2+\gamma)^{M-1}\epsilon^T D_{N-M}Q\epsilon\} + \cdots \end{aligned}$$

Since

$$\epsilon^T Q\epsilon = \gamma - \gamma^*$$

we conclude that

$$Z_{MN} \sim \frac{e^{(N-1)\beta}}{2^{N-1}}(2+\gamma)^{N-1}(\gamma-\gamma^*) \text{ as } \beta\to\infty \text{ for } \gamma\neq\gamma^*.$$

For $\gamma = \gamma^*$ and $2 \le M \le N-2$

$$Z_{MN} \sim \frac{e^{(N-3)\beta}}{2^{N-1}}\{(2+\gamma^*)^{N-M}\epsilon^T QB_{M-1}\epsilon + (2+\gamma^*)^{M-1}\epsilon^T D_{N-M}Q\epsilon\}, \tag{59}$$

with

$$Q = \begin{pmatrix} 1 & \gamma^* \\ 0 & 1-\dfrac{1}{a} \end{pmatrix}.$$

Write

$$B_{M-1} = R^{M-2}S + SR^{M-2} + \sum_{j=1}^{M-3} R^{M-2-j}SR^j\ .$$

Then, in view of (57), we obtain

$$B_{M-1}\epsilon = (M-2)(2+\gamma^*)^{M-3}RS\epsilon + (2+\gamma^*)^{M-2}S\epsilon.$$

Now

$$\epsilon^T QS\epsilon = 2\gamma^* \quad \text{and} \quad \epsilon^T QRS\epsilon = 0$$

so that

$$(2+\gamma^*)^{N-M}\epsilon^T QB_{M-1}\epsilon = 2\gamma^*(2+\gamma^*)^{N-2}. \tag{60}$$

An analogous computation using (58) yields

$$(2+\gamma^*)^{M-1}\epsilon^T D_{N-M}Q\epsilon = -2\gamma^*(\frac{1}{a}-1)(2+\gamma^*)^{N-2}. \tag{61}$$

Therefore we obtain (30) after substituting (60) and (61) into (59), and recalling that $B_0 = D_0 = 0$.

REFERENCES

[1] D. G. Aronson and H. F. Weinberger, *Nonlinear diffusion in population genetics, combustion and nerve propagation*, in Lecture Notes in Mathematics, Springer-Verlag, Berlin, 446, (1975), pp. 5–49.

[2] ———, *Multidimensional nonlinear diffusions arising in population genetics*, Adv. Math., 29 (1978), pp. 33–76.

[3] S. Boitano, E. R. Dirksen, and M. J. Sanderson, *Intercellular propagation of calcium waves mediated by inositol trisphosphate*, Science, 258 (1992), pp. 292–295.

[4] A. C. Charles, C. C. G. Naus, D. Zhu, G. M. Kidder, E. R. Dirksen, and M. J. Sanderson, *Intercellular calcium signalling via gap junctions in glioma cells*, J. Cell Biol., 118 (1992), pp. 195–201.

[5] M. O. Enkvist and K. D. McCarthy, *Activation of protein kinase C blocks astroglial gap junction communication and inhibits the spread of calcium waves*, J. Neurochem., 59 (1992), pp. 519–526.

[6] T. D. Hassinger, P. B. Guthrie, P. B. Atkinson, M. V. L. Bennett, and S. B. Kater, *An extracellular signaling component in propagation of astrocytic calcium waves*, Proc. Nat. Acad. Sci., 93 (1996), pp. 13268–13273.

[7] T. J. Lewis and J. P. Keener, *Wave-block in excitable media due to regions of depressed excitability*, SIAM J. Appld. Math., 61 (2000), pp. 293–316.

[8] H. McKean, *Nagumo's equation*, Adv. Math., 4 (1970), pp. 209–223.

[9] H. P. McKean, *Stabilization of solutions of a caricature of the Fitzhugh-Nagumo equation (2)*, Comm. Pure & Appld. Math., 37 (1984), pp. 299–301.
[10] H. P. McKean and V. Moll, *Stabilization to the standing wave in a simple caricature of the nerve equation*, Comm. Pure & Appld. Math., 39 (1986), pp. 485–529.
[11] H. G. Othmer, *A continuum model for coupled cells*, J. Math. Biol., 17 (1983), pp. 351–369.
[12] J. P. Pauwelussen, *Nerve impulse propagation in a Branching nerve system: A simple model*, Physica, 4D (1981), pp. 67–88.
[13] J. Rinzel and J. B. Keller, *Travelling wave solutions of a nerve conduction equation*, Biophys. J., 13 (1973), pp. 1313–1337.
[14] J. Rinzel and D. Terman, *Propagation phenomena in a bistable reaction-diffusion system*, SIAM J. Appld. Math., 42 (1982), pp. 1111–1137.
[15] J. Sneyd and J. Sherratt, *On the propagation of calcium waves in an inhomogeneous medium*, SIAM J. Appl. Math., 57 (1997), pp. 73–94.
[16] J. Sneyd, M. Wilkins, A. Strahonja, and M. J. Sanderson, *Calcium waves and oscillations driven by an intercellular gradient of inositol (1,4,5)-trisphosphate*, Biophys. Chem., 72 (1998), pp. 101–109.
[17] P. A. Spiro and H. G. Othmer, *The effect of heterogeneously-distributed ryR channels on calcium dynamics in cardiac myocytes*, Bull. Math. Biol, 61 (1999), pp. 651–681.
[18] A. Verkhratsky, R. K. Orkand, and H. Kettermann, *Glial calcium: homeostasis and signaling function.*, Physiol. Rev., 78 (1998), pp. 99–141.
[19] S. Yagodin, L. A. Holtzclaw, and J. T. Russell, *Subcellular calcium oscillators and calcium influx support agonist-induced calcium waves in cultured astrocytes*, Mol. and Cell. Biochem., 149 (1995), pp. 137–144.
[20] S. V. Yagodin, L. Holtzclaw, C. A. Sheppard, and J. T. Russell, *Nonlinear propagation of agonist-induced cytoplasmic calcium waves in single astrocytes*, J. Neurobiol., 25 (1994), pp. 265–280.
[21] J. Yang, S. Kalliadasis, J. H. Merkin, and S. K. Scott, *Wave propagation in spatially distributed exciable media*, SIAM J. Appl. Math, 63 (2002), pp. 485–509.

Received November 2004; revised April 2005.

E-mail address: `othmer@math.umn.edu`
E-mail address: `don@ima.umn.edu`
E-mail address: `nman@rice.edu`